

# Geological Survey of Finland

**Bulletin 339**

**Development of deformation, metamorphism  
and metamorphic blocks in eastern  
and southern Finland**

**Edited by Kalevi Korsman**

**Geologian tutkimuskeskus  
Espoo 1986**



1886

1986

**Geological Survey of Finland, Bulletin 339**

**DEVELOPMENT OF DEFORMATION, METAMORPHISM AND  
METAMORPHIC BLOCKS IN EASTERN  
AND SOUTHERN FINLAND**

Edited by  
**KALEVI KORSMAN**

with 32 figures and 16 tables

**GEOLOGIAN TUTKIMUSKESKUS  
ESPOO 1986**

**Korsman, K. 1986. (ed.)** Development of deformation, metamorphism and metamorphic blocks in eastern and southern Finland. *Geological Survey of Finland, Bulletin* 339. 58 p, 32 figures, 16 tables.

U-Pb (zircon) and K-Ar (hornblende & biotite) isotope data are given for the Archaean Lapinlahti—Varpaisjärvi area. The zircon ages of the enderbites of the high-grade block are 2.68—2.69 Ga, and the hornblende (K-Ar) ages are similar. The hornblende data outside the block also show similar ca. 2.65 Ga blocking ages, whereas the corresponding zircon dates of the tonalitic melanosome of the banded granite gneiss are of middle Archaean age, 3.1 Ga.

Three faults trending in different directions intersect each other in the Tervo area. The oldest deformational event was a strong areal tectono-metamorphic process. The first fault deformation was accompanied by intense recrystallization and granitization. The second fault deformation resembles the earlier one, but the recrystallization is not so clear. The youngest of the fault deformations differs from the others in its cataclastic structures, which are suggested to be products of deformation nearer the erosion level than that of the older ones.

Progressive metamorphism in the Rantasalmi—Sulkava area was preceded by a metamorphic phase associated with D1 deformation. The decomposition reaction of muscovite and the associated crystallization of potassium feldspar and sillimanite took place during the second deformation phase as did the growth of andalusite porphyroblasts in the less metamorphosed portion of the area. The crystallization of cordierite accompanying the decomposition of biotite occurred during the D3 deformation, but garnet and cordierite did not attain equilibrium until after the D3 deformation.

Samples taken from the garnet-cordierite gneiss and from the migmatizing potassium granite in the Turku area suggest that at the culmination of metamorphism the temperature was c. 800°C and the pressure 5—6 kilobars. The rocks have undergone very intense retrograde metamorphism, which is seen as zoning in garnet and as crystallization of andalusite and biotite during the retrogressive stage.

Key words: granulites, deformation, metamorphism, block structures, evolution, Precambrian, Finland.

*Geological Survey of Finland, SF-02150 ESPOO, Finland*

ISBN 951-690-238-3

ISSN 0367-522X

Vammala 1986 Vammalan Kirjapaino Oy

## CONTENTS

Jorma Paavola: A communication on the U-Pb and K-Ar age relations of the Archaean basement in the Lapinlahti—Varpaisjärvi area, central Finland	7
Matti Pajunen: Deformation analysis of cataclastic structures and faults in the Tervo area, central Finland .....	16
Kalevi Korsman and Timo Kilpeläinen: Relationship between zonal metamorphism and deformation in the Rantasalmi—Sulkava area, southeastern Finland	33
Pentti Hölttä: Observations on metamorphic reactions and PT conditions in the Turku granulite area .....	43



## PREFACE

Recent studies have shown that metamorphism reflects many facets of crustal evolution and structure. Areas metamorphosed in granulite facies are in a particularly good position in attempts to unravel crustal evolution. Compiled in the present volume are studies dealing with the evolutionary history of the granulite areas in southern Finland and their immediate environment.

Jorma Paavola discusses the evolution of the granulite block at Varpaisjärvi, located in the Archaean granite gneiss area in eastern Finland, on the basis of zircon, hornblende and biotite ages. The active stage of the granulite block and its environment was between 3100 Ma and 2700 Ma ago, which is a rather long span compared with that in the corresponding Proterozoic areas, in which the evolution started about 1900 Ma ago and the conditions of granulite facies were reached 1800 Ma ago. The data reported in this study also corroborate the earlier concept that the evolution of the Archaean crust was already far advanced when granulite facies metamorphism took place at Varpaisjärvi 2700 Ma ago.

Metamorphic block structure has been established for the Proterozoic bedrock in the marginal area of the Archaean granite gneisses in eastern Finland. Matti Pajunen has studied the age relations of the deformation phases pertinent to the block structure in the Tervo migmatite area. His study shows that only the oldest deformation phase observed in the area is associated with the progressive stage of metamorphism. The deformations that followed the oldest stage were related to fragmentation, retrograde metamor-

phism and granitization of the bedrock. In contrast, Kalevi Korsman and Timo Kilpeläinen have noted that the strongest metamorphic pulse did not develop until after the D3 stage in the Rantasalmi—Sulkava area in southeastern Finland. There is no discrepancy in the observations, however, because, as shown by the former studies, the metamorphism of the Sulkava granulite area is younger by about 100 Ma than the metamorphism of the granulite facies in the environment of the Tervo area.

Pentti Hölttä has investigated the crystallization history of the Turku granulite area in southwestern Finland, where metamorphism took place at high temperature ( $T = 800^{\circ}\text{C}$ ) and at relatively low pressure ( $P = 5\text{--}6\text{ kb}$ ). Hölttä has paid special attention to the cooling stages of the granulite area. On account of retrograde metamorphism, the crystallization conditions that prevailed during the culmination of the metamorphism are only reflected in the compositions of the big garnets.

The studies in the present volume were carried out mainly at the Geological Survey of Finland. The study by Matti Pajunen, which was conducted in co-operation with the University of Turku and the Geological Survey, is part of a project financed by the Academy of Finland dealing with metamorphic reactions between the silicate and sulphide phases. All the studies in the volume are on subjects related to the programme 'Metamorphism and Geodynamics' (No. 235) of the IGCP project.

*Kalevi Korsman*  
Editor



# A COMMUNICATION ON THE U-Pb AND K-Ar AGE RELATIONS OF THE ARCHAEOAN BASEMENT IN THE LAPINLAHTI— VARPAISJÄRVI AREA, CENTRAL FINLAND

by  
**Jorma Paavola**

**Paavola, J. 1986.** A communication on the U-Pb and K-Ar age relations of the Archaean basement in the Lapinlahti—Varpaisjärvi area, Central Finland. *Geological Survey of Finland, Bulletin 339*. 7—15, 3 figures and 3 tables.

U-Pb (zircon) and K-Ar (hornblende & biotite) isotope data are given for the Archaean Lapinlahti—Varpaisjärvi area. The age problem of the area is twofold: the Varpaisjärvi metamorphic high-grade block on one hand and the related lower-grade rocks outside the block on the other. The zircon ages of the enderbites of the high-grade block are 2.68—2.69 Ga, the hornblende (K-Ar) ages being nearly the same. The hornblende (K-Ar) data outside the block also show similar ca. 2.65 Ga blocking ages, whereas the corresponding zircon (U-Pb) dates of the tonalitic melanosome of the banded granite gneiss are of middle Archaean age, 3.1 Ga.

Two biotite (K-Ar) determinations, from inside and outside the block, give ages of 2.39 and 2.09 Ga, respectively. The possible causes and significance of these ages are discussed briefly.

Key words: gneisses, enderbite, absolute age, U/Pb, zircon, K/Ar, Archean, Lapinlahti, Varpaisjärvi, Finland

*Geological Survey of Finland  
Regional Office P.O. Box 237 SF-70101 Kuopio, Finland*

## INTRODUCTION

The western zone of the Archaean basement in eastern Finland, known as the Iisalmi block (Väyrynen, 1939), is fractured (Kauppinen, 1973; Paavola, 1984a), and consists predominantly of tonalitic — trondhjemitic granitoids and migmatites with amphibolitic bands, inclusions and horizons.

In the course of bedrock mapping (1 : 100 000 scale) of this Archaean area, some U-Pb determinations on zircons were performed at the Branch of Isotope Geology of the Geological Survey of Finland.

K-Ar dating of the hornblendes and biotites of the same rock samples was done at the Univer-



sity of Leeds.

The few existing zircon determinations of basement rocks inside the Iisalmi block give ages of ca. 2.7 Ga (A. Huhma, 1976; Neuvonen *et al.*, 1981). These ages represent the time of an important thermal event. The Archaean high-grade metamorphic rocks in the Varpaisjärvi block area with their well-preserved granulite facies mineral assemblages are considered mainly to be products of this thermal pulse (Paavola, 1984a). Granulite facies rocks of still earlier metamorphism are also possible. The block obviously represents a deeper erosion level than the surroundings, and its enderbitic rocks give very concordant zircon (U-Pb) ages of 2.68 Ga (Neuvonen *et al.*, 1981, pp. 116—117). The initial  $^{176}\text{Hf}/^{177}\text{Hf}$  ratio of the zircon of this rock has been

determined by Patchett *et al.* (1981). The ratio plots quite close to the chondritic Hf growth curve, indicating a mantle heterogeneity of some degree for Lu/Hf.

No age determinations are yet available from the adjoining pyroxene amphibolite material.

The new zircon (U-Pb) data reported in this communication mainly concern the banded tonalitic — trondhjemitic basement in the Lapinlahti area (Fig. 1), where the rocks are considered to be lower-grade equivalents of the aforementioned high-grade rocks (Paavola, 1984a).

The enderbitic sample A979 is from inside the Varpaisjärvi block (Fig. 1), and its age is previously unpublished. This age (2.69 Ga) coincides with the ages of the related rocks (samples A843 & A844) mentioned above.

## SAMPLES

The area discussed in this communication yielded six samples for zircon (U-Pb) determinations: three (A843, A844, A979) from the enderbitic basement in the metamorphic high-grade block and three (A645, A76, A937) from outside that block. Four (KA001, KA007, KA008, KA010) of the six rock samples were also submitted to hornblende (K-Ar) determination. Only two of them (KA008, KA010) were analysed for biotite (K-Ar) ages. All the sampling localities are marked on the map in Figure 1. The locations are listed more accurately in Table 1.

The enderbitic basement has a leucodioritic — quartz dioritic composition with plagioclase (50—70 %), hornblende, biotite, hypersthene and quartz as the main minerals. Apatite and magnetite are also relatively abundant. The rock is generally banded or heterogeneous but in places very homogeneous and massive. The aforementioned three dating samples (A843, A844, A979)

are from the massive portions.

The samples A76, A937 and A645 are from the banded tonalitic — trondhjemitic basement. Two of them (A76, A937; ca. 4.5 km apart) consist of relatively homogeneous, foliated tonalitic — quartz dioritic melanosome material with plagioclase, quartz, hornblende and biotite as principal minerals. Some indications of an earlier higher metamorphic grade exist here, too, such as the obvious pseudomorphs after pyroxene, which are totally occupied by secondary minerals.

Sample A645 represents trondhjemitic — leucogranitic neosome material closely associated with the outcrop of sample A937. It was emplaced during a later deformational phase, and nebulitic palaeosome relicts are visible in places. The leucosome material consists mainly of plagioclase, K-feldspar and quartz with small amounts of relict and secondary minerals.

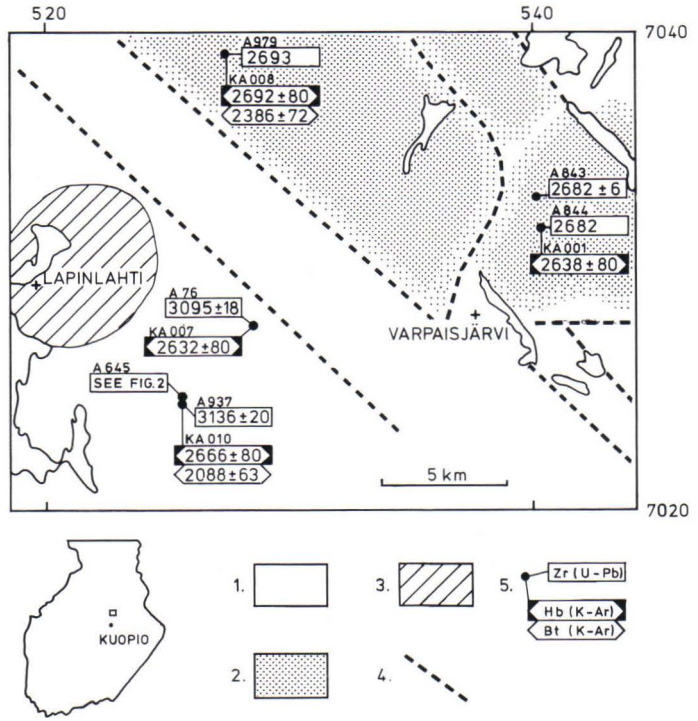


Fig. 1. The locations and sample numbers of the coexisting zircon(U-Pb), hornblende(K-Ar) and biotite(K-Ar) datings in the Lapinlahti—Varpaisjärvi area. Symbols: 1. Archæan tonalitic — trondhjemitic basement, 2. related Archæan high-grade metamorphic rocks, 3. Proterozoic plutonic rock, 4. fracture or fault, 5. sample location and the associated ages.

## RESULTS

The U-Pb isotope results of the zircon fractions are listed in Table 2, and a summary of the U-Pb zircon data from the Lapinlahti—Varpaisjärvi area is plotted in Figure 2.

The four zircon fractions from the enderbite sample (A979) are almost concordant, three of them plotting very close to the concordia line.

The same concordance is characteristic of the earlier enderbite samples (A843, A844), too (Neuvonen *et al.*, 1981; Paavola, 1984b). The accepted age for sample A979 is 2693 Ma.

The zircon crystals of the fine-grained population are euhedral, bright and acicular (L/B ~ 5) with normal colouring. The pyramid surfaces are

Table 1. Summary of U-Pb ages from the Lapinlahti—Varpaisjärvi area.

Sample and location	Number of fractions	Concordia intercepts		Reference
		Upper	Lower	
<i>Enderbitcs</i>				
A843, Paloiskylä, Varpaisjärvi	3	2682 ± 6	595 ± 180	Neuvonen <i>et al.</i> , 1981; Paavola, 1984b This study
A844, Palokangas, Varpaisjärvi	1			
A979, Lampiensalmi, Lapinlahti	4	2693		
<i>Tonalitic melanosome</i>				
A76, Romonmäki, Lapinlahti	7	3095 ± 18	851 ± 232	» »
A937, Kiikkukallio, Lapinlahti	3	3136 ± 20	1459 ± 411	» »
<i>Trondhjemitic leucosome</i>				
A645, Kiikkukallio, Lapinlahti	4			» »

Table 2. U-Pb isotopic data. Decay constants: Jaffey *et al.* (1971).

Zircon fraction d = density Ø = size in µm HF = preleached in HF	Concentration		Atom ratios						Accepted	
	µg/g		measured	blank corrected			corrected for blank and common lead; age (Ma)			age
	<sup>238</sup> U	<sup>206</sup> Pb radio- genic	<sup>206</sup> Pb  <sup>204</sup> Pb	<sup>206</sup> Pb  <sup>204</sup> Pb	<sup>207</sup> Pb  <sup>206</sup> Pb	<sup>208</sup> Pb  <sup>206</sup> Pb	<sup>206</sup> Pb  <sup>238</sup> U	<sup>207</sup> Pb  <sup>235</sup> U	<sup>207</sup> Pb  <sup>206</sup> Pb	(Ma)
A76-Romonmäki, Lapinlahti; qtz.diorite gneiss										
A d>4.6; Ø<160 HF	250.8	125.36	9784	10498	.23351	.14800	.5778 ±30 2939	18.517 ±98 3016	.23243 ±7 3069	3095
B 4.3<d<4.6	413.8	203.34	2972	3007	.23729	.12803	.5680 ±29 2899	18.289 ±96 3005	.23354 ±9 3076	
C d>4.3; Ø>160 HF; uncrushed	351.8	177.79	6660	6949	.23528	.11985	.5841 ±30 2965	18.815 ±99 3032	.23365 ±3 3077	
D 4.2<d<4.3 HF; uncrushed	464.4	230.08	8357	8737	.23305	.13837	.5726 ±30 2918	18.295 ±97 3005	.23176 ±16 3064	
E 4.0<d<4.1 Ø<160; HF uncrushed	713.6	330.12	2682	2711	.23105	.12389	.5347 ±28 2761	16.723 ±89 2919	.22686 ±15 3030	
F 4.0<d<4.1 Ø>70 long crystals	725.0	327.02	927.8	935.6	.24095	.17165	.5214 ±27 2704	16.449 ±87 2903	.22884 ±6 3044	
G 4.0<d<4.1 Ø>70	740.7	322.49	1150	1155	.23466	.14018	.5032 ±29 2627	15.597 ±91 2852	.22480 ±12 3015	
A645-Kiikkukallio, Lapinlahti; trondhjemitic neosome										
A d 4.3; Ø>160	470.3	217.97	5882	6904	.21010	.09568	.5357 ±38 2765	15.39 ±11 2839	.20839 ±25 2893	
B d>4.3 70<Ø<160 long crystals	500.0	229.52	4970	5504	.20739	.10671	.5305 ±53 2743	15.01 ±15 2815	.20524 ±38 2868	
C d>4.3 70<Ø<160 round crystals	461.4	200.97	3456	4764	.19107	.08947	.5034 ±43 2628	13.09 ±12 2685	.18854 ±37 2729	
D d>4.3 70<Ø<160 vague	477.9	214.27	7525	8217	.20123	.14898	.5182 ±60 2691	14.27 ±17 2768	.19978 ±13 2824	
A937-Kiikkukallio, Lapinlahti; tonalitic melanosome										
A d>4.6	125.9	65.88	6923	7765	.24041	.14000	.6046 ±68 3048	19.92 ±23 3087	.23897 ±17 3113	3136
B 4.3<d<4.6	195.3	100.49	8222	9079	.23816	.11099	.5946 ±40 3008	19.42 ±13 3063	.23693 ±16 3099	
C 4.3<d<4.6 HF; uncrushed	191.7	99.93	15696	18744	.23874	.10935	.6025 ±45 3039	19.78 ±15 3080	.23814 ±28 3107	
A979-Lampiansalmi, Lapinlahti; enderbitic basement										
A d>4.6	83.1	37.28	10012	14137	.18526	.15854	.5187 ±48 2693	13.19 ±13 2693	.1844 ±4 2693	2693
B 4.3<d<4.6 HF; uncrushed	116.1	52.38	24650	58641	.18540	.16665	.5214 ±47 2704	13.31 ±12 2702	.18519 ±20 2700	
C 4.3<d<4.6	119.5	54.10	37055	427061	.18513	.17109	.5233 ±44 2712	13.35 ±12 2704	.18510 ±44 2699	
D 4.3<d<4.6	97.7	41.87	25715	117059	.18553	.16616	.4951 ±33 2592	12.66 ±9 2654	.18543 ±21 2702	

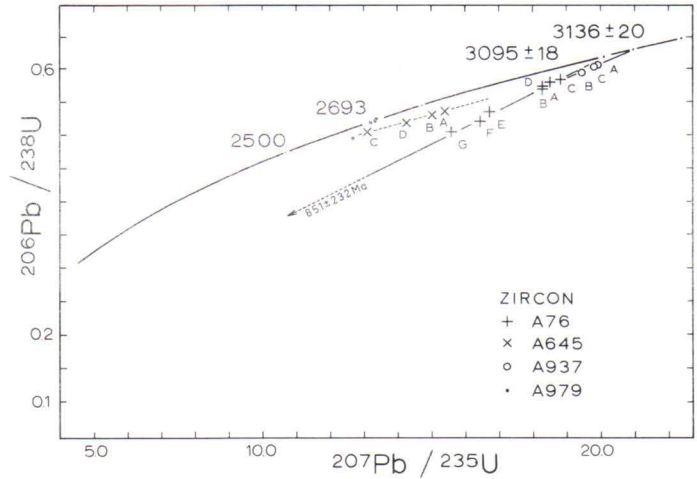


Fig. 2. Concordia plot for the zircons from the Lapinlahti—Varpaisjärvi area.

not well exhibited nor are the edges very sharp. Large crystals are not acicular.

The zircons of sample A76 are rather homogeneous and euhedral (L/B ~ 3—4) with bright crystal faces. The crystals are prismatic but not as well developed as in undeformed rocks. Rounded crystals are not met with either.

The zircons of sample A937 constitute different density fractions: the zircons with  $d > 4.6$  are predominantly bright and L/B ~ 1.5, whereas only some of the zircons with  $d = 4.3—4.6$  are entirely bright. These lighter zircons also have round-

ish edges (L/B ~ 1.5—2). The lightest zircons ( $d = 4.0—4.2$ ) are dark brown, rounded and large without any crystal faces.

The zircon population of the adjoining leucosome material (A645) is expectedly heterogeneous, and so it does not yield an unambiguous age, although the old U-Pb inheritance is obvious. A mixed population is the most likely explanation, because the discordant ages are due to the points that lie approximately on a straight line on the concordia diagram (Fig. 2). The fraction giving the oldest age ( $T_{207Pb/206Pb} = 2893$  Ma) has crys-

Table 3. K-Ar dates from the Lapinlahti area, Central Finland.

Sample	NO.	%K	Vol <sup>40</sup> Ar rad. ccSTP/g × 10 <sup>-5</sup>	% <sup>40</sup> Ar rad.	Age (Ma)
Hornblende	KA001	1.23 ± 0.004	28.872 28.518	98.5 98.3	2638 ± 80
Hornblende	KA007	1.41 ± 0.013	32.617 32.471	98.9 98.9	2632 ± 80
Hornblende	KA008	1.05 ± 0.010	25.451 25.198	98.3 98.9	2692 ± 80
Hornblende	KA010	1.32 ± 0.007	31.291 31.356	98.4 98.6	2666 ± 80
Biotite	KA008	7.43 ± 0.01	143.00 143.98	98.4 99.2	2386 ± 72
Biotite	KA010	7.14 ± 0.02	108.85 109.73	99.2 99.1	2088 ± 63

$\lambda_{\beta}$  :  $4.962 \times 10^{-10} \text{yr}^{-1}$   
 $\lambda_{\alpha}$  :  $0.581 \times 10^{-10} \text{yr}^{-1}$   
 $^{40}\text{K}$ : 0.01167 atom%

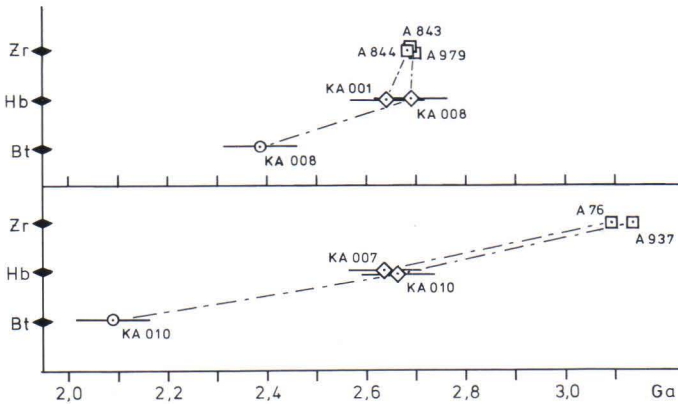


Fig. 3. Mineral dating from the Lapinlahti—Varpaisjärvi area on the time scale. Symbols: square = zircon(U-Pb) age, diamond = hornblende(K-Ar) age and circle = biotite(K-Ar) age. Upper section: Enderbitites from the Varpaisjärvi high-grade metamorphic area. Lower section: Tonalitic melanosome of the banded basement from the Lapinlahti area.

tals larger than  $160\ \mu\text{m}$ . The transparent, brownish and euhedral crystals have L/B ca. 3—4. The analysed fraction (4.53 mg) includes some light-coloured fragments. Fraction B consists of euhedral, long (L/B ~ 6), brownish and transparent needles with bright crystal faces. 1.50 mg of roundish, subhedral, brownish and mostly transparent crystals were picked up (fraction C). L/B is 2—1.5 and the few crystal faces visible show that this ratio represents the original habitus. The material was not completely free from long needles (B). Fraction D consists of crystals difficult to determine. This sample was not studied for lower density fractions. The four fractions analysed were heavier than  $4.3\ \text{g}/\text{cm}^3$  and the content of uranium varied from 461 to  $500\ \mu\text{g}/\text{g}$ .

This type of mixed population has been found

in Finland, e.g. in rheomorphic dykes within layered intrusions of 2440 Ma age.

The K-Ar (hornblende & biotite) isotope results and ages are shown in Table 3.

Figure 3 summarizes the present dating results and gives a general idea of basic differences between the enderbites of the Varpaisjärvi block and the tonalitic melanosome of the banded basement in the Lapinlahti area in relation to their past principal tectono-thermal events (uplift/erosion, reheating, metamorphism, etc.).

As to the present rocks and dates, a large number of correlative features have been reported from other Archaean shields, e.g. the Pikwitonei subprovince in Manitoba (Ermanovics and Wanless, 1983).

## DISCUSSION

It is important to note that all the hornblende ages are close to each other and that they are also very close to those of the zircons of enderbites (about the same within limits of error). This indicates extensive regional thermal activity about 2.7 Ga ago.

The blocking temperature of the hornblende (K-Ar) system is generally accepted to be 450—

$500^\circ\text{C}$  (e.g. Jäger and Hunziker, 1979; Mattinson, 1982). However, it is evident that the blocking temperature of the dry, hypersthene bearing (granulite facies) rocks is still higher (e.g. Berger and York, 1981; Deutsch and Steiger, 1985). The surprising coincidence with the present zircon and hornblende ages of the enderbites indicates the same, even though cooling after the 2.7

Ga thermal activity would have been rather fast. Hence, no appreciable thermal pulse has affected the enderbite rocks in the Varpaisjärvi area since 2.7 Ga. The well preserved thermoremanent magnetism of these rocks is consistent with the same idea (Neuvonen *et al.*, 1981). The exceptionally high biotite (K-Ar) age, 2.39 Ga (sample KA008) also indicates stable conditions in the enderbite basement during the post-Archaean.

The age determinations on biotite from the Finnish Archaean basement performed so far have yielded ~1.75 Ga (Wetherill *et al.*, 1962; Kouvo and Tilton, 1966). The ages of biotites from the Proterozoic rocks are about the same, 1.70–1.77 Ga (Wetherill *et al.*, 1962; Korsman *et al.*, 1984). The granulite area in Lapland seems to have some correlative features with the present area, giving the somewhat high age of 1.88 Ga (Wetherill *et al.*, 1962).

As stated, a dry milieu may raise blocking temperatures and thus hinder the younging of biotite at temperatures higher than ca. 300°C, which is considered to be the approximate blocking temperature of biotite (see Jäger and Hunziker, 1979; Mattinson, 1978).

Thus, according to the only biotite (K-Ar) age from the enderbites, no Jatulian effect can really be seen, although a swarm of pyroxene diabases, believed to be Jatulian (Neuvonen *et al.*, 1981), cut the high-grade rocks. However, the aforementioned »dry milieu protection» seems to be a good explanation for the high biotite age.

The results (samples A76, A937 and KA007, KA010) outside the high-grade block differ from those above. The biotite (K-Ar) determination (KA010) gives a clearly lower age (2.08 Ga) than that of enderbite (KA008). This blocking age of biotite can most easily and naturally be attributed to reheating caused by Jatulian diabases. Unlike in the enderbite rocks, the reheating was evidently able to reset the biotite clocks in the more hydrous environments of the basement.

As stated, the K-Ar method on hornblende (KA007, KA010) gives blocking ages very similar to those of enderbites, while the zircon U-

Pb method on the tonalitic — quartz dioritic melanosome yields the middle-Archaean ages (3.09 and 3.14 Ga) given above. It is possible that these ages refer to the time of primary crystallization of the tonalitic magma. In any case, the zircon, unlike the hornblende of the same rock, has not been affected by the 2.7 Ga thermal activity.

It is obvious that additional isotope studies will reveal older ages than 2.7 Ga for the high-grade rocks of the Varpaisjärvi block as well, especially because no age determinations are yet available from the palaeosome material (e.g. two-pyroxene amphibolite).

The 3.1 Ga zircon dates are notably older than the ca. 2.8–2.7 Ga ages from the Archaean granitoids of eastern Finland obtained so far (e.g. Kouvo and Tilton, 1966; Hyppönen, 1983; Martin *et al.*, 1984; Luukkonen, 1985). The Kelovaaara quartzite, in Kainuu, exhibits old detrital zircon material (Hyppönen, 1983). The ages are highly discordant but give the upper intersection with concordia at 2996 Ma. According to the diffusion model the age would be more than 3100 Ma.

From the Koitelainen area, Lapland, true, Kröner *et al.* (1981) report zircon(U-Pb) and Sm-Nd data giving the age of 3.1 Ga. They attribute this age to the emplacement of the original tonalitic — trondhjemitic intrusive body. Jahn *et al.* (1984) confirm the results and maintain that the initial  $^{143}\text{Nd}/^{144}\text{Nd}$  ratio indicates even earlier (3.5–3.6 Ga) separation of magma from the upper mantle.

H. Huhma (1985) gives Sm-Nd model ages calculated on the basis of a primitive mantle. The Archaean metapelite from Ilomantsi, easternmost Finland, gives a model age of  $3.08 \pm 0.08$  Ga, indicating that at least part of the material is from an older source than the present granitoids in the environment.

Lobikov and Lobach-Zhuchenko (1980) have also reported 3.1 Ga zircon(U-Pb) age data on granites from the Palaya Lamba area, Central Karelia.

The high dates are, in a way, unexpected, especially for the fractured Iisalmi block area, which has clearly been more exposed to post-Archaean influences than the eastern zone of the basement. On the other hand, the conspicuous fractures and faults of the area might have acted as principal escaping surfaces of tensional and compressive forces and protected the blocks in between.

Väyrynen (1939, pp. 31—33) was the first to express the idea of a western push forcing the Iisalmi block to thrust towards the southeast.

One obvious Proterozoic continental break-up concerning the detachment of the Iisalmi block has been demonstrated by Kontinen (in press).

According to him, the detachment culminated in the rifting and formation of oceanic crust 1970 Ma ago.

The 3.1 Ga ages from the Lapinlahti area differ conspicuously from all other zircon ages from the eastern Presveco Karelian basement of Finland. It is, however, possible that corresponding ages have not yet been recorded elsewhere or that they might have been rejuvenated, e.g. by stronger deformation, deeper erosion, more hydrous circumstances, or some other process. Hence, it cannot be concluded, on the ground of the age determinations performed so far, that a basic age difference really does exist between the eastern and western basement granitoids.

#### ACKNOWLEDGEMENTS

I owe special thanks to Dr. O. Kouvo for the collaboration resulting in the zircon age determinations. He also read the manuscript critically, suggesting useful improvements. I am also grateful to Dr. D. C. Rex of the University of Leeds

for the K-Ar isotope analyses.

Thanks are also due to Mr. P. Kallio and Mrs. T. Neuvonen, who performed the mineral separation, and to Mr. J. Eskelinen, who helped to process the present material.

#### REFERENCES

- Berger, G. W. & York, D., 1981.** Geothermometry from  $^{40}\text{Ar}/^{39}\text{Ar}$  dating experiments. *Geochim. Cosmochim. Acta* 45, 795—811.
- Deutsch, A. & Steiger, R. H., 1985.** Hornblende K-Ar ages and the climax of Tertiary metamorphism in the Lepontine Alps (south-central Switzerland): an old problem reassessed. *Earth Planet. Sci. Lett.* 72, 175—189.
- Ermanovics, I. F. & Wanless, R. K., 1983.** Isotopic age studies and tectonic interpretation of Superior Province in Manitoba. *Geol. Surv. Can.*, paper 82—12.
- Huhma, A., 1976.** New aspects to the geology of the Outokumpu region. *Bull. Geol. Soc. Finland* 48, 5—24.
- Huhma, H., 1985.** Provenance of some Finnish sediments. *Geologi* 2, 23—25.
- Hyppönen, V., 1983.** Kallioperäkarttojen selitykset. *Lehdet* 4411, 4412 ja 4413, Ontojoen, Hiisijärven ja Kuhmon kartta-alueiden kallioperä. English summary: Pre-Quaternary rocks of the Ontojoki, Hiisijärvi and Kuhmo map sheet areas. Suomen geologinen kartta 1 : 100 000.
- Jaffey, A. H., Flynn, K. F., Glendenin, L. E., Bentley, W. C. & Essling, A. M., 1971.** Precision measurements of half-lives and specific activities of  $^{235}\text{U}$  and  $^{238}\text{U}$ . *Phys. Rev. C* 4, 1889—1906.
- Jäger, E. & Hunziker, J. C. (eds.), 1979.** Lectures in isotope geology. Springer—Verlag, Berlin, 312p.
- Jahn, B., Vidal, P. & Kröner, A., 1984.** Multi-chronometric ages and origin of Archaean tonalitic gneisses in Finnish Lapland: a case for long crustal residence time. *Contrib. Mineral. Petrol.* 86, 398—408.
- Kauppinen, H., 1973.** Iisalmen alueen lohkorakenteista. M. Sc. thesis in the archives of geology and mineralogy, University of Turku, 102p.
- Kontinen, A., in press.** An Early Proterozoic ophiolite — the Jormua mafic-ultramafic complex, north-eastern Finland. *Precambrian Res.*

- Korsman, K., Hölttä, P., Hautala, T. & Wasenius, P., 1984.** Metamorphism as an indicator of evolution and structure of the crust in eastern Finland. *Geol. Surv. Finland, Bull.* 328, 40p.
- Kouvo, O. & Tilton, G. R., 1966.** Mineral ages from the Finnish Precambrian. *J. Geol.* 74, 421—442.
- Kröner, A., Puustinen, K. & Hickman, M., 1981.** Geochronology of an Archaean tonalitic gneiss dome in northern Finland and its relation with an unusual overlying volcanic conglomerate and komatiitic greenstone. *Contrib. Mineral. Petrol.* 76, 33—41.
- Lobikov, A. F. & Lobach-Zhuchenko, S. B., 1980.** Isotopic age of granites Palaya Lamba greenstone belt, Karelia. *Dokl. Earth Sci. Sections*, vol. 250, 197—200.
- Luukkonen, E., 1985.** Structural and U-Pb isotopic study of late Archaean migmatitic gneisses of the Presvecokareliides, Lylyvaara, eastern Finland. *Trans. R. Soc. Edinb. Earth Sci.*, 76, 401—410.
- Martin, H., Auvray, B., Blais, S., Capdevila, R., Hameurt, J., Jahn, B. M., Piquet, D., Querre, G. & Vidal, Ph., 1984.** Origin and geodynamic evolution of the Archaean crust of eastern Finland. *Bull. Geol. Soc. Finland* 56, (1—2), 135—160.
- Mattinson, J. M., 1978.** Age, origin and thermal histories of some plutonic rocks from the Salinian block of California. *Contrib. Mineral. Petrol.* 67, 233—245.
- Mattinson, J. M., 1982.** U-Pb »blocking temperatures» and Pb loss characteristics in young zircon, sphene and apatite. The geological society of America. 95th annual meeting. Abstracts with programs. Abstract n:o 08946, vol. 14.
- Neuvonen, K. J., Korsman, K., Kouvo, O. & Paavola, J., 1981.** Paleomagnetism and age relations of the rocks in the Main Sulphide Ore Belt in Central Finland. *Bull. Geol. Soc. Finland*, 53—2, 109—133.
- Paavola, J., 1984a.** On the Archean high-grade metamorphic rocks in the Varpaisjärvi area, Central Finland. *Geol. Surv. Finland Bull.* 327, 33p.
- Paavola, J., 1984b.** Kallioperäkartojen selitykset — Explanation to the maps of Pre-Quaternary rocks. Lehti — Sheet 3334, Nilsjä. Geological map of Finland, 1 : 100 000, 57p.
- Patchett, P. J., Kouvo, O., Hedge, C. E. & Tatsumoto, M., 1981.** Evolution of continental crust and mantle heterogeneity: Evidence from Hf isotopes. *Contrib. Mineral. Petrol.* 78, 279—297.
- Väyrynen, H., 1939.** On the geology and tectonics of the Outokumpu ore field and region. *Bull. Comm. Geol. Finlande* 124, 91p.
- Wetherill, G. W., Kouvo, O., Tilton, G. R. & Gast, P. W., 1962.** Age measurements on rocks from the Finnish Precambrian. *J. Geol.* 70, 74—88.



# DEFORMATION ANALYSIS OF CATACLASTIC STRUCTURES AND FAULTS IN THE TERVO AREA, CENTRAL FINLAND

by  
**Matti Pajunen**

**Pajunen, M., 1986.** Deformation analysis of cataclastic structures and faults in the Tervo area, Central Finland. *Geological Survey of Finland, Bulletin 339*. 16—31, 10 figures.

Three faults trending in different directions intersect each other in the Tervo area. Their deformation style, age relations and relations to metamorphism and granitization are interpreted.

The oldest deformational event was a strong regional tectonic-metamorphic process characterized by penetrative mineral foliation and upper amphibolite facies metamorphism. The first, and regionally most important, fault deformation occurred in the directions of 315—320° and was accompanied by intense recrystallization and granitization. The second, local fault deformation trends N-S. Microstructurally it resembles the previous one, but the recrystallization is not so clear. The youngest of the strong fault deformations also trends roughly N-S, but it differs from the others in its cataclastic structures, which are suggested to be products of deformation nearer the erosion level than that of the older ones. Hence, in the Tervo area, we can distinguish one strong, regional tectono-metamorphic episode, which was followed by at least three fractural fault movements, thus causing the crustal block structure typical of the Ladoga-Bothnia Bay zone.

Key words: cataclasites, mylonites, faults, deformation, metamorphism, lineaments, Proterozoic, Tervo, Finland.

*Institute of Geology and Mineralogy,  
University of Turku, 20500 Turku, Finland.*

## INTRODUCTION

Cataclastic deformation is a process in which a rock granulates and breaks under stress in a fault or shear movement (Higgins 1971). It is usually defined as a dynamic deformation without chemical changes (e.g. Gary *et al.* 1974), al-

though nowadays evidence abounds of changes in bulk chemical, mineral and isotopic compositions under shearing (Kerrich *et al.* 1980, Brodie 1981, Etheridge & Cooper 1981, Hickman & Glassley 1984 and Passchier 1985). The changes

are mainly caused by fluid migration (Brodie 1981, Etheridge & Cooper 1981 and Hickman & Glassley 1984).

According to Ramsay (1980), the shear zones are either brittle, brittle-ductile or ductile, and commonly the basic component of strain is a heterogeneous simple shear. The style of deformation and the cataclastic rock types change with increasing depth (Sibson 1977 & Ramsay 1980). In the near-surface fault zones the most typical cataclastic rocks are noncohesive fault breccias and fault gouges produced by brittle deformation. With increasing depth the cohesion increases in random-fabric crush breccias, producing microbreccias and cataclasites. The deep-zone cataclastic rocks are plastically deformed, cohesive and fluxion-structured rocks of the protomylonite-mylonite-ultramylonite and mylonite gneiss-blastomylonite series. All cataclastic rock types are gradational to each other, and poly-

cataclastic structures are typical (Higgins 1971 & Sibson 1977).

The investigated area is situated in the Ladoga-Bothnia Bay zone, which is a NW-SE-trending area, about 100 km wide of intense fracturing, faulting and shearing in Central Finland. The zone is characterized by crustal block structure (e.g. Marttila 1976 and Korsman *et al.* 1984). Despite the number of publications dealing with the importance and nature of the zone, the cataclastic rocks associated with it have rarely been discussed. The main purpose of the present paper is to describe and analyse in detail the cataclastic structures and age relations of deformation in a small area in Tervo, called the Tervo area in the following (Fig. 1). The material for this study was collected when I was working as a field assistant for the Geological Survey of Finland. All the laboratory work was done at the University of Turku and the Geological Survey.

## REGIONAL GEOLOGY

In the Ladoga-Bothnia Bay zone the topographic lineaments parallel the direction of the zone. The lineaments indicate faults, which have been considered old, mainly Precambrian, fracture zones (Härme 1961), but which are still seismically active zones of weakness (Penttilä 1964 and Talvitie 1971). According to Paarma (1962), the present uplift of mosaic-like blocks takes place along these old zones. Observations of the epicentres of present earthquakes in the areas of topographic lineaments trending 270–275°, 305–310°, 325° and 0–5° also support the concept of late movements (Talvitie 1971 and 1975). The blocks have uplifted at variable velocities in different places. Lehtovaara (1976) found that, as a result of more rapid uplift of the crust in the southwestern part of the zone, the fission track ages of apatites in the Haukivesi area are older in the northeastern part than in the southwestern part of the zone. A marked ne-

gative gravity anomaly in the direction of the zone (Honkasalo 1962) is at least partly due to granitization in the fractured and sheared bedrock, for example, in the Tervo area (Elo 1983).

The bedrock in the study area consists of two lithological units: the Savo schist belt in the east and the granitoid complex of Central Finland in the west. The contact between the units is indefinite because of faulting, blocking and granitization (Figs. 1 and 2). These phenomena are also evident on geological map sheet 3313, Vesanto (Pääjärvi 1985).

Korsman *et al.* (1984) stress the differences in the metamorphic structure of the crust between the progressively metamorphosed Rantasalmi–Sulkava area and the Rautalampi–Pielavesi–Pihtipudas area, which are characterized by metamorphic blocks bounded by faults. These fault lines coincide with seismic block boundaries, some of which penetrate the crust, as indi-

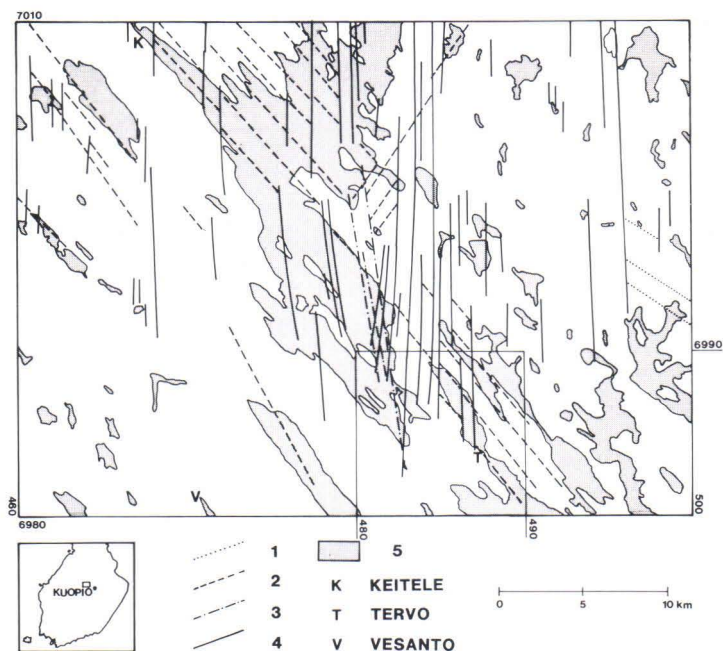


Fig. 1. Magnetic lineaments (1—4, see explanations in the text) and lakes (5) of map sheet 3313. The Tervo area (geological map in Figure 2) is marked in the figure.

cated in the SVEKA profile (Luosto *et al.* 1982). According to Korsman *et al.* (1984), the orogenic phase that occurred about 1880 Ma ago in the Rautalampi and Pielavesi areas was related to a tensional event. The granulite facies metamorphism in the Pielavesi and Rautalampi blocks is related in both time and space to deep-seated pyroxene granitoid magmatism, which was preceded by an earlier orogenic event about 1930—1920 Ma ago as demonstrated by the ages of the Kirkkosaari, Rastinpää (Korsman *et al.* 1984) and Kettuperä gneisses (Helovuori 1979). Metamorphic block structures of the same kind have been described by Paavola (1984) from the Archaean basement area of Varpaisjärvi.

The supracrustal rocks within the gneissic tonalites are the oldest rocks in the Tervo area. Their origin, if known, is volcanic or volcanic-sedimentary. Phlebitic or stromatic neosome of the banded gneisses is thronhjemitic or, rarely, granitic in composition. Primary bedding is seldom visible. The most common gneisses are intermediate, locally cummingtonite- and garnet-bearing biotite-plagioclase-hornblende or biotite-

hornblende gneisses. Amphibolites are rare. Epidote, chlorite and relict hypersthene are encountered occasionally. The difference between the true supracrustal rocks and the banded cataclastic rocks is sometimes difficult to verify.

The most common rocks in the area are metamorphosed gneissic tonalites in the east and porphyritic granitoids in the west. The oldest infracrustal rocks are gabbro and diorite fragments in the tonalites. Chemically, the tonalites are calc-alkaline rocks indicating the gabbro-thronhjemitic trend of Barker & Arth (1976), Arth *et al.* (1978) and Hunter (1979). The composition varies from thronhjemitic to tonalitic and quartz dioritic. Some types have abundant cummingtonite and garnet. Banding, ghost-like inclusions and thronhjemitic migmatization are typical.

Orthopyroxene-bearing, Hautomäki-type gabbros are younger than the tonalites but older than the porphyritic granitoids. They are tholeiitic orthocumulates with plagioclase and bronzitic orthopyroxene as cumulus and diopsidic clinopyroxene, biotite and accessory phases as intercumulus minerals. In the central part of the Hau-

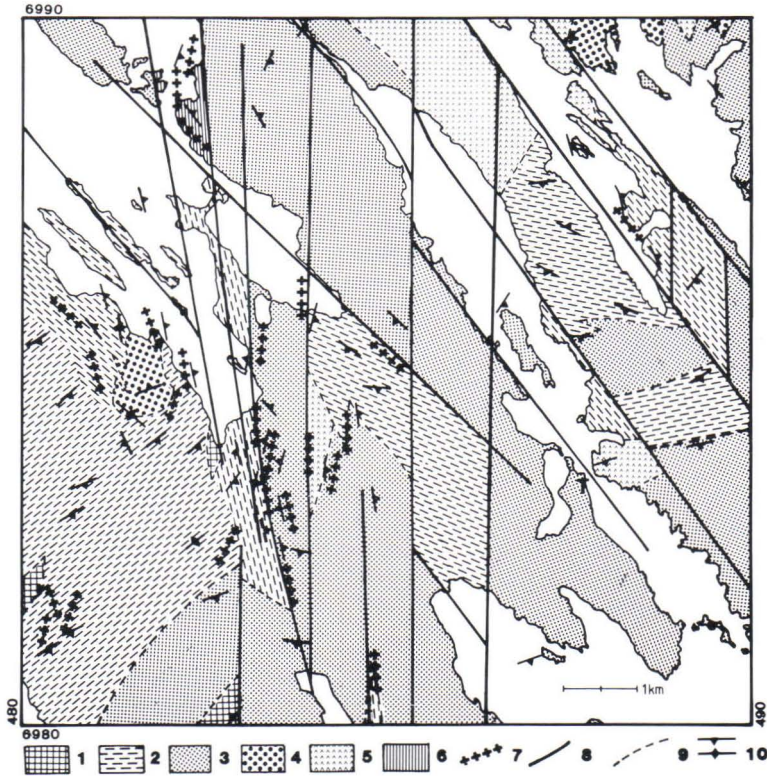


Fig. 2. Geological map of the Tervo area 1) granite and granodiorite, 2) porphyritic granitoid, 3) tonalite, 4) Hautomäki-type gabbro, 5) biotite-plagioclase gneiss, 6) hornblende gneiss, 7) cataclastic zones, 8) magnetic lineaments, 9) contact and 10) foliation.

tomäki stock, uralitization of pyroxenes is intense. The rocks are mostly medium-grained, but fine-grained and pegmatitic types have also been met with. The only orientation in the gabbros is weak magmatic and sporadic cataclastic foliation.

The contacts with the porphyritic granitoids are always gradational because granitization has caused the growth of K-feldspar in the contact areas. The porphyritic granitoids are coarse-grained with pronounced foliation that is frequently cataclastic. The composition varies from granitic to granodioritic. K-feldspar is always secondary microcline in the investigated samples. The average size of the porphyroblasts is about 3 cm and their abundance varies in the range 5–50 %. They have usually grown in the direction of schistosity, and in cataclastic types they

are rounded, giving rise to augen gneiss texture. Locally, the old structure of the pregranitization rocks is visible, for example, where the remnants of older tonalites have been preserved. The youngest igneous rocks are pegmatitic and aplitic granite dykes.

The Kinturi-Iisvesi fault, described by Korsman *et al.* (1984), is deformed by younger faults in the study area. In the Pihtipudas—Pielavesi area, the fault coincides with the metamorphic isograd indicating a change from low amphibolite facies in the eastern part of the Pihtipudas block to the retrograde area metamorphosed in the stability field of K-feldspar-sillimanite. In the Rautalampi area, the fault coincides with the isograd between stabilities of muscovite and garnet-cordierite/hypersthene (Korsman *et al.* 1984). In the study area, the mineral assemblage

ges of rocks indicate amphibolite facies metamorphism. In supracrustal rocks and tonalites, the relict hypersthene and the retrograde cummingtonite after it indicate that the culmination of metamorphism was near the conditions of granulite facies. The retrograde phenomena associ-

ated with the post-metamorphic cataclastic deformation are rather limited. The most typical alteration process is the biotitization of amphiboles and pyroxenes; chloritization and epidotization occur occasionally.

### Cataclastic rocks

The cataclastic rocks are named according to the classification of Higgins (1971) which is based on the presence or absence of primary cohesion and fluxion structures, the degree of neomineralization and recrystallization, which are nowadays explained as syntectonic processes (Bell & Etheridge 1973 and White *et al.* 1980), and the size and amount of fragments and porphyroclasts. Although the classification is descriptive, the structures also give information on deformational conditions and depth (Sibson 1977).

The majority of the cataclastic rocks in the study area belong to the protomylonite-mylonite-ultramylonite and mylonite gneiss-blastomylonite series. Rocks with breccia structures have been met with in long-lived sutures usually trending 335–345°. Polycataclastic structures are common.

The width of the zones of brecciated, cataclastic rocks varies in sutures from 0.5 to 1 m. They deform previously mylonitized rocks. The noncohesive type consists of rusty, green fault gouge rich in micas. Matrix of secondary origin, such as zeolite, has been detected in narrow fissures. Cohesive microbreccias and cataclasites are in the same brecciated zones as narrow seams; their matrix is composed of the primary rock-forming minerals. The angular fragments are mostly feldspar. Retrograde phenomena such as chloritization of biotite and rusty pigmentation and seritization of feldspar are pronounced. The brecciated rocks are the products of late, near-surface brittle deformation.

Fluxion structure is formed by warping of in-

competent matrix around competent porphyroclasts or rounded fragments. Porphyroclastic minerals are plagioclase, microcline, garnet and hornblende. Microcline and garnet are also true porphyroblasts. Rock fragments are common in protomylonites, but they have been broken down in mylonites and ultramylonites. Pressure shadows adjoining the porphyroclasts and fragments are common. Protomylonites are the most widespread cataclastic rocks in the area. The primary rock can often be recognized under the protomylonitic structure. Mylonites are concentrated in seams some metres in width. Porphyroclasts, which are mostly monomineralic with unstrained inclusions, are 0.3–0.5 mm in size. Compositional banding is typical with light plagioclase- and quartz-rich and dark biotite-rich layers; in mylonitic rocks hornblende is commonly altered into biotite. Drag folds are generally associated with strongly deformed zones. Ultramylonites are only narrow seams of less than 10 cm in mylonitic rocks. Their porphyroclasts are about 0.1 mm in size and the matrix has been thoroughly reduced in grain size. In mylonite gneisses and blastomylonites, the most pronounced phenomena are strong recrystallization of quartz and biotite, and formation of microcline porphyroblasts locally. The recrystallization and neomineralization are more intense in granitic and gabbroic rocks than in intermediate rocks. The cataclastic structures in the Kinturi—Iisvesi fault zone are chiefly mylonite gneissic to blastomylonitic. The neomineralization, especially the biotitization of amphiboles, has markedly increased the ductility of the rock mass.

## MAGNETIC LINEAMENTS

The interpretation of lineaments on geophysical maps forms the basis for further study when solving the succession of deformation of strongly faulted areas. The fracture zone trending NW-SE is a conspicuous tectonic feature that characterizes the whole area of the Baltic Shield (Strömberg 1976). The Ladoga-Bothnia Bay zone is clearly visible on the aerial photographs as lineaments, e.g. on the maps of Härme (1961) and Talvitie (1971), and on satellite images, as reported by Kuosmanen *et al.* (1978). The true nature of the zone is still unclear.

In the present study, the lineaments have been defined from the grey tone interpretation of low altitude aeromagnetic map sheet 3313 at a scale of 1 : 100 000 (Geol. Surv. Finland 1982). The topographic lineaments are unreliable because of the intense orientation of glacial structures, although the topographic features, e.g. lakes, seem to coincide rather well with the magnetic lineaments (Fig. 1). The straight ruptures in magnetic anomalies have been attributed to faults, which can be distinguished as narrow seams with low magnetic gamma values between highly magnetized areas. The strongly oriented magnetic anomaly field, for example, to the north of the Tervo area in Fig. 1, represents an almost penetra-

tive shear or fault movement.

The map area is divided into three units according to the type of magnetic anomaly. The eastern part is heterogeneous and minor featured; the western part is rather uniformly magnetized except for the high level area in its eastern margin; and the central northern part contains a highly magnetized triangle-shaped area. Between these blocks there is a well oriented and heterogeneous magnetic anomaly field suggesting sheared and faulted bedrock. In the eastern block the lineaments indicating true faults are difficult to distinguish from those caused by earlier tectonic or stratigraphic features. The same problem arises in the northern block. In the west only a few lineaments are there are visible, but they are easily identified as faults.

In the boundary areas of the blocks it is even possible to identify the age relations of the lineaments, and they have been numbered in the order of decreasing age. The directions of the lineaments are 305° (1 in Fig. 1), 315–320° and 30° (2), 350° (3) and 0–10° (4). The cataclastic cleavages in the Tervo area frequently trend 315°, 20–30°, 350° and 0–10° (Fig. 2), and they coincide with magnetic lineaments.

## DEFORMATION HISTORY OF THE TERVO AREA

The factors that are effective in deformation are the differences in competence of the rock types, the prevailing PT conditions, the amount of fluid phase and the strain rate (Hobbs *et al.* 1976). Cataclastic structures are products of rapid movements. The depth of deformation also influences the ultimate result (cf. Sibson 1977). Felsic and intermediate rocks abound in the study area. They behave rather competently, and structures typical of rigid body deformation, such as

faults, which are concentrated in narrow seams or in wider shear zones, are typical. Earlier deformation events can be discerned in the well preserved blocks between the shear zones. The directions of foliation are quite homogeneous within the blocks, but the blocks may differ considerably from each other (Fig. 2).

Difficulties accumulate when the fault or shear zones become older. Many of the faults show signs of reactivation, and interpretation of the

ages of the polycataclastic structures formed may be problematic. In this study, the deformation phases have been distinguished on map, outcrop and microscopic scale, and misleading reactivation structures, such as cataclastic seams, were rejected in the interpretation of age relations. The directions of faults are usually rather uniform, but differences in competences of rocks may cause local variations. The direction of slip of fault and the type of deformation are good indicators of fault generation. A big problem in the interpretation of the genesis of fault rocks is the uncertainty about the strain rate during faulting, especially in old faults. The geothermal gradient of Precambrian times, from 44°C/km in the Pielesvi area to 45–50°C/km in the Rantasalmi—

Juva area (Korsman *et al.* 1984), has implications for analysis of the depth of deformation. The border between brittle-plastic deformation has been nearer the erosion level than it is nowadays. Further, secondary factors, such as the »apparent foliation» of Obee and White (1985), may be misleading.

The observations of the present study are from a small area and probably do not cover the whole history of deformation. Hence the deformation phases are named according to Hopgood's (1980) recommendation in alphabetical order: the oldest deformation phase is  $D_a$ , the next  $D_b$  and so on. The foliations  $S$ , lineations  $L$ , folds  $F$  and metamorphisms  $M$  have been described in the same order.

### Pre- $D_a$ processes

The oldest identified structure in the Tervo area is the primary bedding,  $S_0$  which displays

strong boudinage and folding of later movements.

### Deformation phase $D_a$

$D_a$  is the most marked deformation phase in the area, and is associated with upper amphibolite facies regional metamorphism. Older deformation structures have not been identified, and it is possible that they have been destroyed by  $D_a$  deformation. Overprints of  $D_a$  deformation have not been identified in the gabbro at Hautomäki.

$F_a$  folds are tight to isoclinal; their hinges are thickened and their limbs thinned. It is common for the boudinated, rootless hinges of folds to »swim» in a more incompetent rock. This kind of fragmentary structure is typical of  $D_a$  deformation.

$S_a$  is the axial foliation of the  $F_a$  folds. It is

penetrative foliation, and the minerals of upper amphibolite facies have grown in the same direction. The basic inclusions and coarse mobilizations of the tonalites and the neosome of the supracrustal rocks are also in the direction of  $S_a$ . K-feldspar porphyroblasts have grown in the  $S_a$  plane in porphyritic granitoids and granitized tonalites in the eastern part of the area. They are either late-tectonic or post-tectonic with  $D_a$ . Texturally  $S_a$  foliation is granoblastic. The structures of  $D_a$  are best preserved in the eastern part of the area.  $S_a$  commonly trends from east to west and dips gently to south or southeast.  $L_a$  is a mineral lineation plunging gently to southeast.

### Deformation phase $D_b$

$D_a$  structures are cut by deformation  $D_b$  (2 in Fig. 1), which is a strong fault deformation (the Kinturi fault) in the direction  $315\text{--}320^\circ$ . Deformational relations indicate that the  $20\text{--}30^\circ$ -trending deformation has also occurred between  $D_a$  and  $D_c$ . The relationships between the deformations causing the  $D_b$  structures are unknown, and in the following they are named  $D_{b1}$  (Kinturi fault direction) and  $D_{b2}$  ( $20\text{--}30^\circ$ ).  $D_{b1}$  is marked by strong orientation of the magnetic field in the western part of the map sheet, but in the detail area its effects are muted because of younger deformations.  $D_{b2}$  is also a strong shear deformation, and it is best visible in the southwestern part of the detail area. Like  $D_{b1}$  it is not visible on the magnetic map except in the northern part of the area, where its true relations to other deformation phases have not been established.

$S_b$  is either a penetrative, cataclastic foliation or it occurs in the cataclastic seams. K-feldspar

porphyroclasts or porphyroblasts of porphyritic granitoids are commonly in the direction of foliation. To the northwest of the Hautomäki gabbro stock the idiomorphic K-feldspar porphyroblasts have been met with on the  $S_{b1}$  foliation plane, implying syn- to post- $S_b$  growth (Fig. 3). Granitic veins along  $S_b$  planes also indicate that contemporaneous granitization occurred with  $D_b$ . The  $D_b$  structures are cut by pegmatitic granite dykes, which in turn are deformed by younger deformation phases. Banding due to biotite-feldspathic and quartzofeldspathic layers and segregation of quartz are typical. Microscopically,  $S_b$  is mylonite gneissic to blastomylonitic foliation, and it is strongly recrystallized and neomineralized. The dip of  $D_b$  is usually subvertical.

The  $D_{b1}$  minor folds are asymmetrical, isoclinal or tight, sometimes intrafolial, commonly indicating dextral movement.  $F_{b1}$  axes plunge to the northwest with an angle of about  $45^\circ$ .  $F_{b2}$

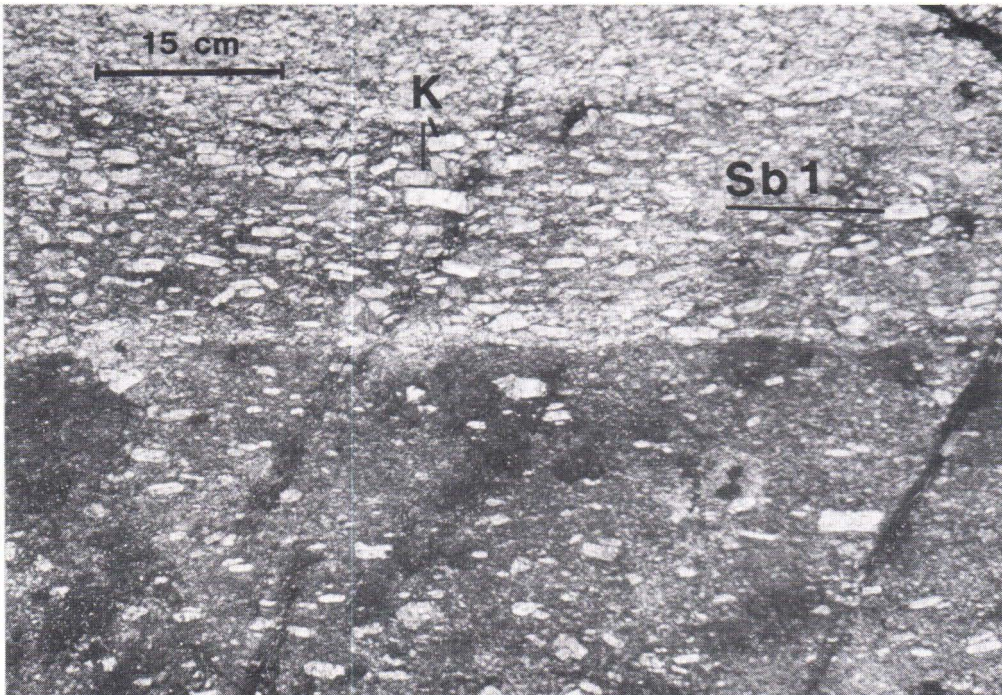


Fig. 3. Granitization associated with deformation phase  $S_{b1}$ . K = K-feldspar.  $x = 6985.10$  and  $y = 481.80$ .



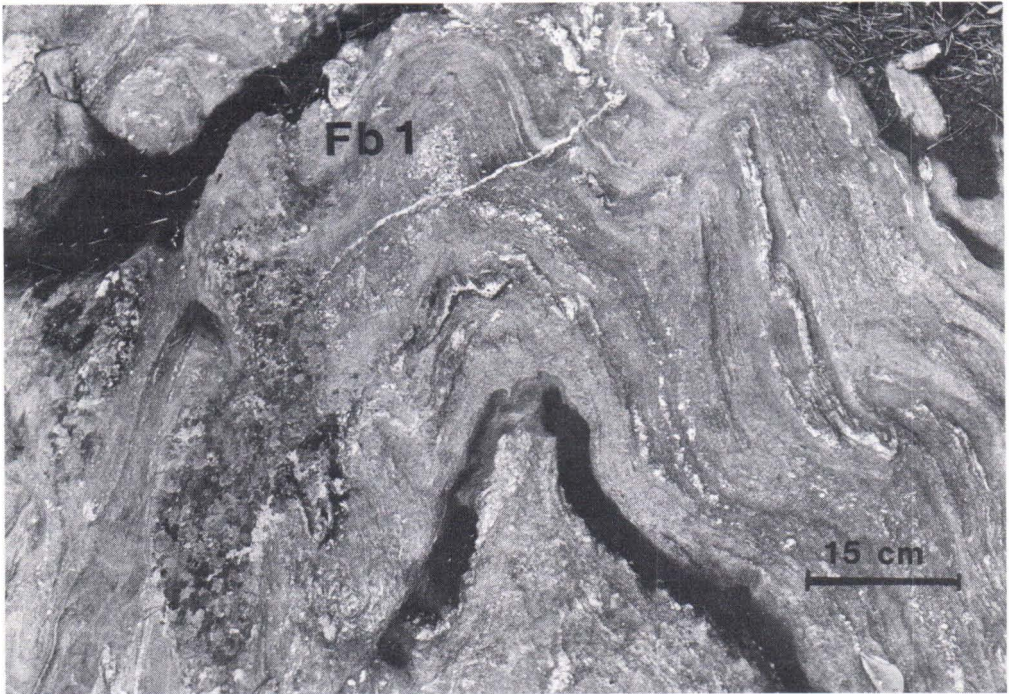


Fig. 4.  $F_{b1}$  folding in blastomylonite.  $x = 6983.10$  and  $y = 483.65$ .

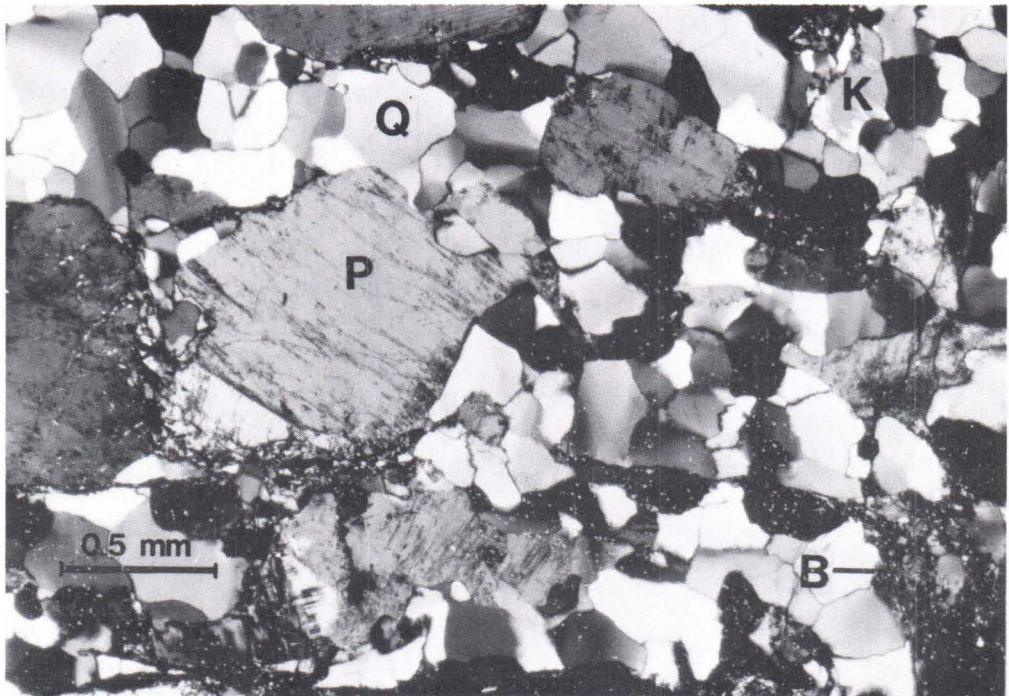


Fig. 5. Strongly recrystallized and neomineralized  $D_{b2}$  mylonite gneiss. B = biotite, K = K-feldspar, P = plagioclase and Q = quartz.  $x = 6981.89$  and  $y = 480.14$ .

folds are tight to isoclinal and their axes plunge gently to the southwest. Some right-handed folds indicate dextral movement.  $F_b$  folds are not markedly thickened in the hinge area (Fig. 4).

The gabbro of Hautomäki was also deformed during  $D_b$ . The granitic fluid that moved during the  $D_b$  deformation phase promoted recrystallization and neomineralization processes (Figs. 3 and 5). Deformation occurred under deep fault zone conditions, as indicated by amphibolite facies mineral assemblages. According to Passchier (1985), deformation under dry conditions may lead to erroneous conclusions, but, in the case under study, fluid pressure was high as demonstrated by the marks of granitization.

As already mentioned, the conjugate nature of  $D_{b1}$  and  $D_{b2}$  has not been proved. If both  $D_{b1}$  and  $D_{b2}$  are right-lateral, the conjugate structure is hardly understood (cf. Hills 1963). Short shear zones,  $S_{b3}$ , cut the  $D_{b1}$  structures of augen gneissic porphyritic granitoids from NE to SW two kilometres northwest of Tervo. The faults, both dextral and sinistral, are shear-faults only some tens of centimetres long like those described by Ramsay (1980) as plastic faults. They gradually die out at their ends by branching into micro-faults. Granitic material has segregated in the most intensely reoriented zones. They have been interpreted to be about the same age as  $D_b$ .

### Deformation phase $D_c$

The clear break in  $D_b$  structures seen on the aeromagnetic map is a local, sharp and narrow fault that has been interpreted as the third de-

formation phase,  $D_c$  (3 in Fig. 1), of the area. In the tonalitic rocks the similarity between the structures of  $D_c$  and  $D_b$  has caused the greatest

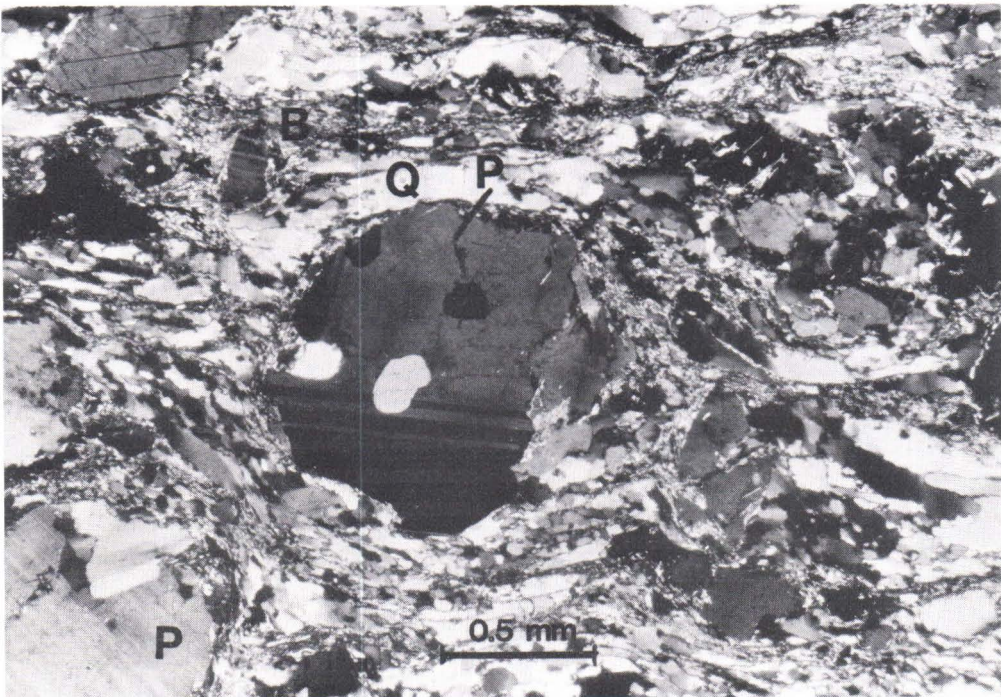


Fig. 6. Rotated porphyroblast in  $D_c$  mylonite. B = biotite, P = plagioclase and Q = quartz.  $x = 6983.65$  and  $y = 483.46$ .

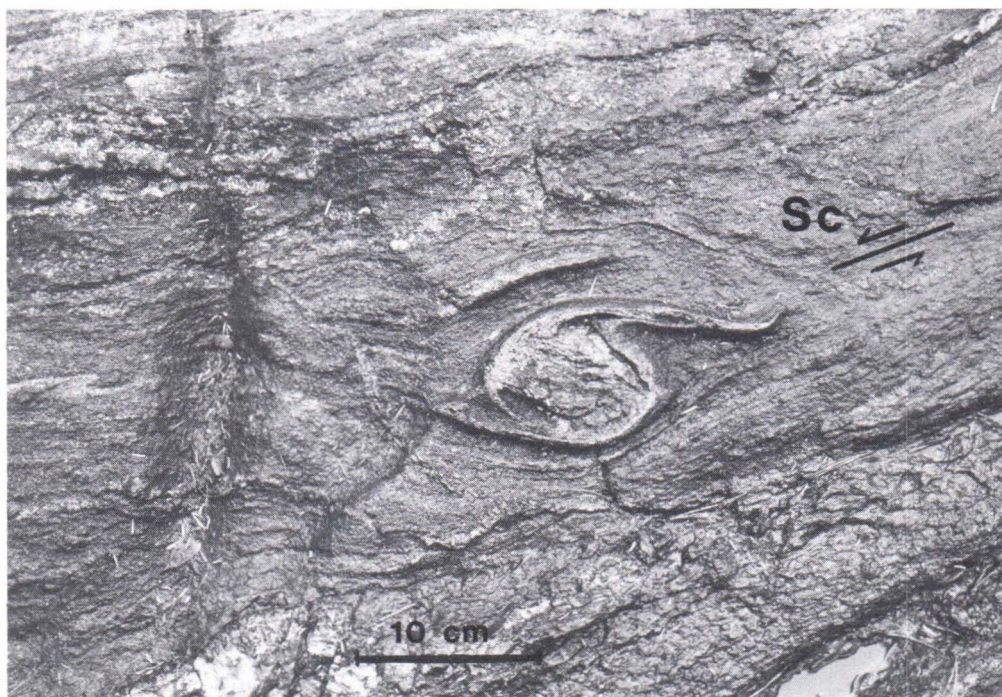


Fig. 7. Rotated fragment in  $D_c$  mylonite.  $x = 6983.44$  and  $y = 483.93$ .

difficulties in the interpretation.

$S_c$  is an almost penetrative cataclastic foliation or it develops into mylonitic and ultramytonitic seams. Texture is cataclastic; protomylonitic to ultramytonitic with some recrystallization and neomineralization (Fig. 6). Banding has developed locally. Segregations of quartz on  $S_c$  planes form quartz plugs lengthened in the direction of lineation  $L_c$ . Cataclastic granitic veins on the  $S_c$  plane have boundinage structures formed under compression. Granitic veins are lacking from the neighbouring fresh rock. Fluidization is thus a syncataclastic process. Some of the veins may be older, turned in the direction of movement as has happened with some pegmatites. Outside the most intense shear zone,  $S_c$

exists only as cataclastic seams that are impossible to distinguish from, say,  $S_b$  or  $S_d$  seams.

$F_c$  folds are asymmetrical drag folds with amplitudes of up to one metre. The axial plane of the folds is only weakly or not at all developed. The  $F_c$  axes are commonly steep.

The slip direction, according to slickenside striations is almost horizontal, indicating mainly strike slip movement, which is mostly sinistral as shown by the rotated porphyroclasts and fragments (Figs. 6 and 7), drag folds and striations.

The textures of  $D_c$  indicate plastic deformation. The late seams with breccia structures show, however, that the movements in the direction of  $D_c$  were long-lived, complicating the age relations of the cataclastic structures.

#### Deformational phase $D_d$

$D_d$  structures deform  $D_a$ ,  $D_b$  and  $D_c$ .  $D_d$  is a N-S-trending fault deformation and shows up cle-

arly on the aeromagnetic map (4 in Fig. 1).

$F_d$  folds are open and upright, and formed

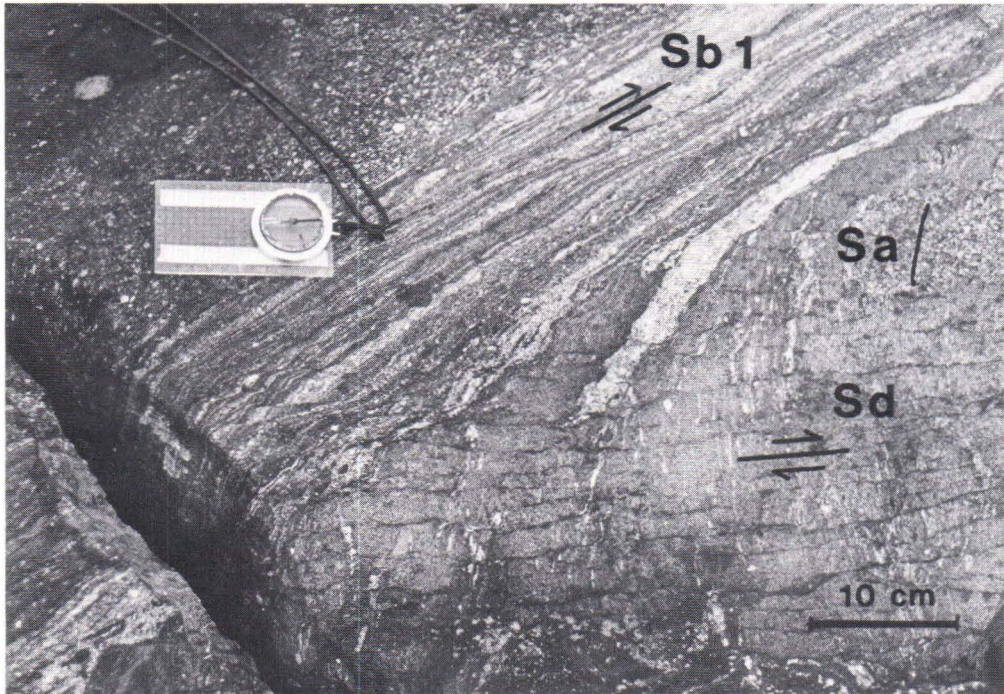


Fig. 8. Relations between deformations  $D_a$ ,  $D_{b1}$  and  $D_d$ .  $x = 6983.68$  and  $y = 483.18$ .

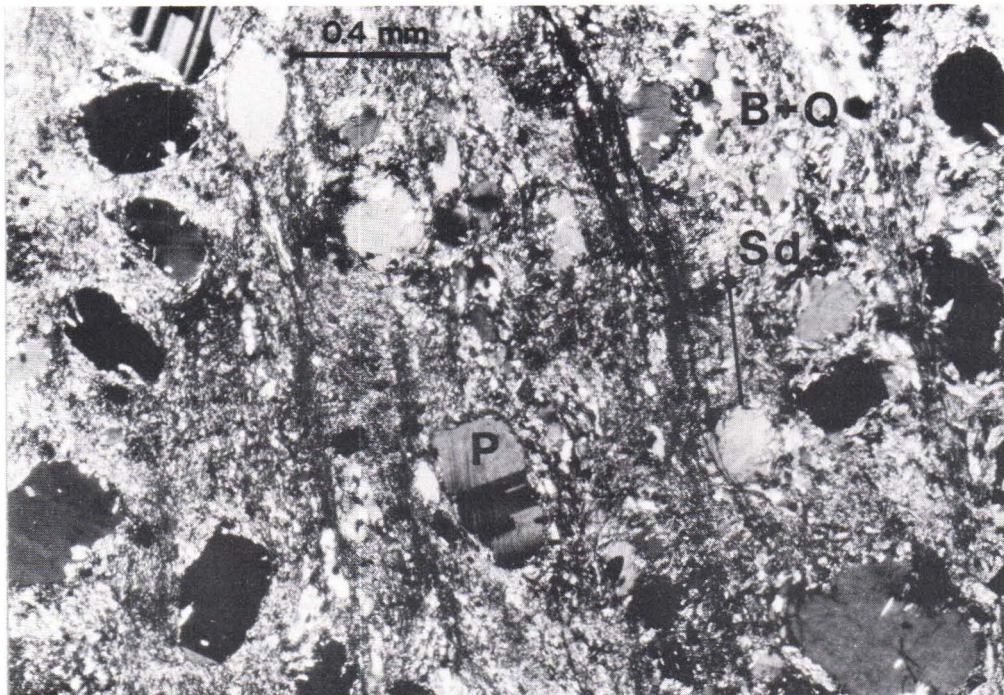


Fig. 9.  $S_d$  fractural cleavage intersects  $D_c$  mylonite. B + Q = biotite and quartz and P = plagioclase.  $x = 6983.68$  and  $y = 483.18$ .

during dextral movement. The  $F_d$  axes dip steeply to southwest, and the slickenside striations  $L_d$  are almost horizontal, also indicating dextral faulting.

Fractural cleavage  $S_d$  has developed locally into mylonitic and ultramylonitic seams (Fig. 8). The older structures are visible between the fractures or cataclastic seams. The width of the preserved space varies from microscopic to some tens of centimetres. Mineral growth associated with the  $D_d$  deformation is rather scant. Microscopically,  $S_d$  is shearing in biotite and oxidation on fractures (Fig. 9). However, when devel-

oped into mylonitic to ultramylonitic seams, typical cataclastic structures, such as porphyroclastic and fluxion structures, have been generated.

As indicators of deformation style and conditions, the  $D_d$  structures appear more brittle than earlier phases. However, the absence of breccia structures allows some estimation of the depth of deformation (cf. Sibson 1977); estimations of the deformational conditions from the mineral assemblages may give erroneous results (cf. Passchier 1985).

### Deformation phase $D_e$

Deformation phase  $D_e$  is an E-W-trending local fault deformation only met with in the western part of the Tervo area. The  $D_e$  deformation intersects structures deformed in the  $D_b$  and  $D_d$

directions. Very open folding of  $S_d$  planes with east-western axial planes also indicates a late structural event.

## SUMMARY OF THE SUCCESSION OF DEFORMATION OF THE TERVO AREA AND DISCUSSION

The succession of deformation of the Tervo area is presented schematically in Fig. 10.

The oldest rocks in the Tervo area are relics of supracrustal rocks existing as inclusions in tonalites. Deformation  $D_a$  is a penetrative, regional tectono-metamorphic event. It is characterized by upper amphibolite facies metamorphism with intense migmatization, isoclinal and often rootless folding, and strong mineral foliation.

Tonalitic magmatism is either pregenetic or syngenetic in relation to  $D_a$ ; in any case, the tonalites were already in a solid state during the culmination of metamorphism and were remobilized during  $D_a$ . Porphyritic granitoids in the eastern part of the area follow the direction of  $S_a$ , but they have not undergone high-grade metamor-

phism as the tonalites have, and they must be regarded either as late- or post- $D_a$ . Porphyritic granitoids are interpreted as products of intense granitization. The Hautomäki-type gabbros intruded at the latest stages of  $D_a$  or after it. They show no signs of  $M_a$  metamorphism, but granitization along the marginal areas is intense. This phase of granitization is accompanied by later cataclastic processes.

The  $D_b$  phase is a dominant fault deformation in the direction of the Kinturi fault, 20–30° and perhaps NE-SW. Distinctive marks of the phase are recrystallization, neomineralization and granitization, causing blastomylonitic to mylonite gneissic structure. This post-metamorphic, right-handed vertical fault with nearly horizon-

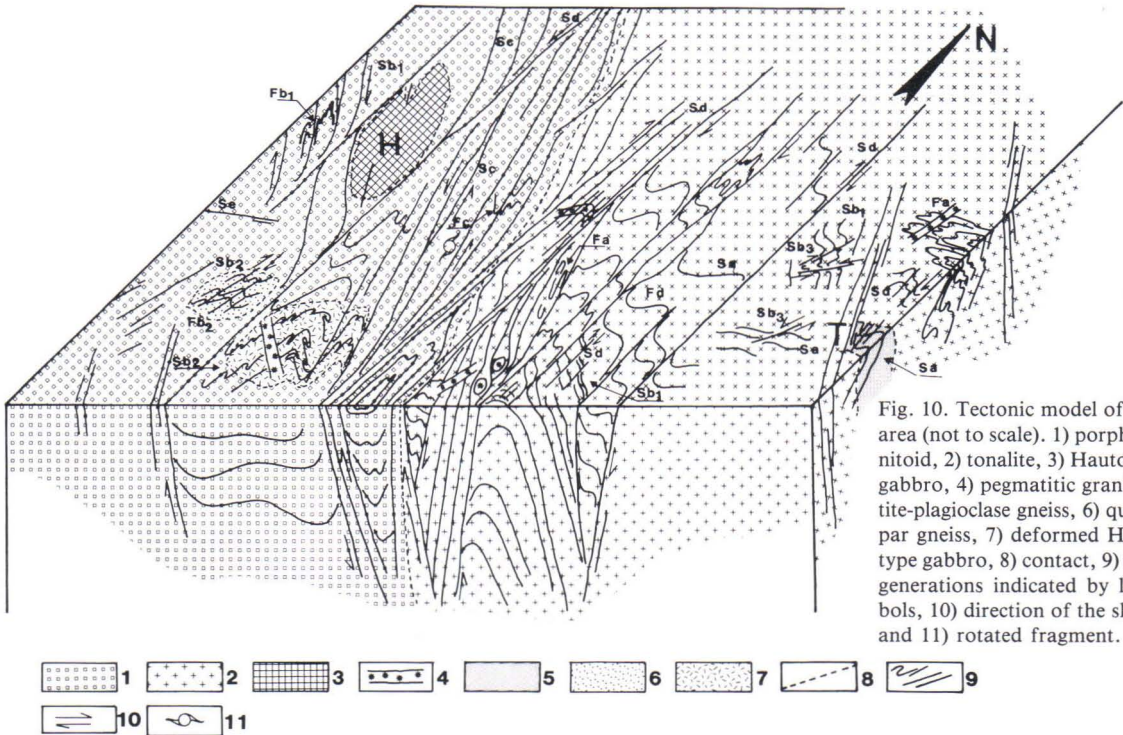


Fig. 10. Tectonic model of the Tervo area (not to scale). 1) porphyritic granitoid, 2) tonalite, 3) Hautomäki-type gabbro, 4) pegmatitic granite, 5) biotite-plagioclase gneiss, 6) quartz-feldspar gneiss, 7) deformed Hautomäki-type gabbro, 8) contact, 9) foliations, generations indicated by letter symbols, 10) direction of the slip of fault and 11) rotated fragment.

tal movement cuts the crust (Luosto *et al.* 1982). The porphyritic granitoids are at least partly syn-genetic with  $D_b$ . According to mineral parageneses and cataclastic structures, the deformation occurred at rather great depth.

$D_c$  is a local, sharp fault-deformation. The fault is commonly vertical and left-handed in the direction of  $350^\circ$ . Recrystallization and neomineralization are not as intense as in the  $D_b$  phase. Plastic deformation structures are dominant, indicating rather great crustal depth during deformation.

$D_d$  is the youngest of the pronounced fault-deformations in the area. It penetrates older structures as right-handed fractural cleavages or mylonitic seams. Fluidization during  $D_d$  is limited, and the mineral parageneses cannot be used as indicators of metamorphic grade. The  $D_d$  deformation occurred at higher crustal levels than the deformations mentioned above.

Difficulties arise when deformation phases of

the Tervo area are correlated with the other deformation analyses from the Ladoga-Bothnia Bay zone area (Parkkinen 1975, Bowes 1980, Gaal 1980, Koistinen 1981, Halden 1982 and Bowes *et al.* 1984). First, the majority of the previous structural analyses were conducted in areas where pelitic, plastically deformed rocks predominate. Second, numbers of previous works describe the deformation of the Presvecokarelian basement or of the Outokumpu nappe area. Third, the structural features of the oldest deformation phases may be very similar in different areas even though their deformation histories differ substantially. The directions of the youngest deformations are preserved over large areas, and they can be used as guide deformations (cf. Hopgood 1980).

Although deformation  $D_a$  is rather similar to the  $D_2$  deformations reported by Koistinen (1981) and Halden (1982), it is not possible to correlate them with each other, because deformati-

on older than  $D_a$  has not been encountered in the Tervo area. Deformation  $D_b$  trends in almost the same direction as  $D_{2c}$  of Koistinen (op. cit.) and Halden (op. cit.). Both Koistinen (op. cit.) and Halden (op. cit.) describe deformation  $D_3$ , which appears as crenulation cleavage in a N-S direction. Deformation  $D_d$  in the Tervo

area has some similarities with  $D_3$ .

Further studies of cataclastic rocks are needed. The regional correlation of cataclastic structures could solve many problems in the crustal development of strongly blocked areas, such as Ladoga Bothnia Bay zone.

### ACKNOWLEDGEMENTS

The material of the present study was collected when I was working as a field assistant for the Geological Survey of Finland, and the paper carried out when I was employed as a research geologist by the Natural Science Research Council of the Academy of Finland. Professor Heikki Pajunen of the University of Turku and Dr. Kalevi Korsman read the manuscript critically, sug-

gesting many improvements and corrections. Mr. Antti Pääjärvi, M.Sc., assisted me in many ways during the field work.

Mrs. Gillian Häkli corrected the English of the manuscript, and the drawings are the work of Miss Aija Siponen.

I wish to thank all of them for their kindly help.

### REFERENCES

- Arth, J. G., Barker, F., Peterman, Z. E. & Friedman, I., 1978.** Geochemistry of the gabbro-diorite-tonalite-trondhjemite suite of southwest Finland and its implications for the origin of tonalitic and trondhjemitic magmas. *J. Petrol.* 19, 289—316.
- Barker, F. & Arth, J. G., 1976.** Generation of trondhjemitic-tonalitic liquids and Archean bimodal trondhjemite-basalt suites. *Geology* 4, 596—600.
- Bell, T. H. & Etheridge, M. A., 1973.** Microstructures of mylonites and their descriptive terminology. *Lithos* 6, 337—348.
- Bowes, D. R., Halden, H. M., Koistinen, T. J. & Park, F., 1984.** Structural features of basement and cover rocks in the eastern Svecokareliides, Finland. *In* Precambrian tectonics illustrated, ed. by Kröner, A. & Greiling, R. E. Schweitzerbart'sche Verlagsbuchhandlung (Nägele u. Obermiller), Stuttgart, 147—171.
- Brodie, K. H., 1981.** Variation in amphibole and plagioclase composition with deformation. *Tectonophysics* 78, 385—402.
- Elo, S., 1983.** Painovoima-anomaloista ja maankuoren rakenteesta SVEKA-profiililla. Esitelmä Geofysiikan IV neuvottelupäivillä Kuopiossa 2. 11. 1983.
- Etheridge, M. A. & Cooper, J. A., 1981.** Rb/Sr isotopic and geochemical evolution of a recrystallized shear (mylonite) zone at Broken Hill. *Contrib. Mineral. Petrol.* 78, 74—84.
- Gaal, G., 1980.** Geological setting and intrusion tectonics of the Kotalahti nickel-copper deposit, Finland. *Bull. Geol. Soc. Finland* 52, 101—128.
- Gary, M., McAfee Jr, R. & Wolf, L. C., 1974.** Glossary of geology. Am. Geol. Institute, Washington, D. C., 805 p.
- Halden, N. M., 1982.** Structural, metamorphic and igneous history at migmatites in deep levels of wrench fault regime, Savonranta, eastern Finland. *Trans. R. Soc. Edinburgh Earth Sci.* 73, 17—30.
- Helovuori, O., 1979.** Geology of the Pyhäsalmi ore deposit, Finland. *Econ. Geol.* 74, 1084—1101.
- Hickman, M. H. & Glassley, W. E., 1984.** The role of metamorphic fluid transport in the Rb-Sr isotopic resetting at shear zones: evidence from Nordre Stromfjord, West Greenland. *Contrib. Mineral. Petrol.* 87, 265—281.
- Higgins, M. W., 1971.** Cataclastic rocks. *U. S. Geol. Surv. Prof. Paper* 687, 97 p.
- Hills, S. E., 1963.** Elements of structural geology. Methuen

- & Co Ltd., London, 483.
- Hobbs, B. E., Means, W. D. & Williams, P., 1976.** An outline of structural geology. John Wiley & Sons, Inc., New York, 571 p.
- Honkasalo, O., 1962.** Gravity survey of Finland in years 1945—1960. Publ. Geod. Inst. 55, 32 p.
- Hopgood, A. M., 1980.** Polyphase fold analysis of gneisses and migmatites. Trans. R. Soc. Edinburgh Earth Sci. 71, 55—68.
- Hunter, D. R., 1979.** Role of tonalitic rocks in crustal development of Swaziland and eastern Transvaal, South Africa. In Trondhjemites, dacites and related rocks, vol. 6, ed. by Barker, F. Elsevier, Amsterdam, 301—322.
- Kerrich, R., Allison, I., Barnett, R. L., Moss, S. & Starkey, J., 1980.** Microstructural and chemical transformations accompanying deformation of granite in a shear zone at Mieville, Switzerland; with implication for stress corrosion cracking and superplastic flow. Contrib. Mineral. Petrol. 73, 221—242.
- Koistinen, T. J., 1981.** Structural evolution of an early Proterozoic strata-bound Cu-Co-Zn deposit, Outokumpu, Finland. Trans. R. Soc. Edinburgh Earth Sci. 72, 115—158.
- Korsman, K., Hölttä, P., Hautala, T. & Wasenius, P., 1984.** Metamorphism as an indicator of evolution and structure of the crust in eastern Finland. Geol. Surv. Finland, Bull. 328, 40 p.
- Kuosmanen, V., Paarma, H. & Tuominen, H. V., 1978.** Laatokan-Perämeren-vyöhyke osana suuremmasta systeemistä. Laatokan-Perämeren malmivyöhykesymposium Ota-niemessä, Geologijaosto, Vuorimiesyhdistys, 70—83.
- Luosto, U., Lanne, E., Korhonen, H., Guterch, A., Grad, M., Materzok, R., Pajchel, J., Perhuc, E. & Yliniemi, J., 1982.** Results of the deep seismic soundings of the earth's crust on profile SVEKA. Proceedings of the 18th general assembly of the ESC, Leeds.
- Marttila, E., 1976.** Evolution of the Precambrian volcanic complex in the Kiuruvesi area, Finland. Geol. Surv. Finland, Bull. 283, 109 p.
- Obee, H. K. & White, S. H., 1985.** Faults and associated fault rocks of the Southern Arunta block, Alice Springs, Central Australia. J. Struct. Geol. 7, 701—712.
- Pääjärvi, A., 1985.** Pre-Quaternary rocks, Sheet 3313, Vesaanto. Geological Map of Finland, 1 : 100 000.
- Paarma, H., 1964.** On the tectonic structure of Finnish basement, especially in the light of geophysical maps. Fennia 89, 33—36.
- Paavola, J., 1984.** On the Archean high-grade metamorphic rocks in the Varpaisjärvi area, Central Finland. Geol. Surv. Finland, Bull. 327, 33 p.
- Passchier, C. W., 1985.** Water-deficient mylonite zones — An example from Pyrenee. Lithos 18, 115—127.
- Penttilä, E., 1964.** Some remarks on earthquakes in Finland. Fennia 89, 23—28.
- Ramsay, J. G., 1980.** Shear zone geometry: a review. J. Struct. Geol. 2, 83—99.
- Sibson, R. G., 1977.** Fault rocks and fault mechanism. J. Geol. Soc. London 122, 191—213.
- Strömberg, A. G. B., 1976.** A pattern of tectonic zones in the western part of the European platform. Geol. Fören. Förh. 98, 227—243.
- Talvitie, J., 1971.** Seismotectonics of Kuopio region, Finland. Bull. Comm. geol. Finlande 248, 41 p.
- , 1975. Fractures, dynamic model and Ni-Cu mineralized basic intrusives in Central Finland. Geol. Surv. Finland, Report of Investigation No. 10, 3—12.
- White, S. H., Burrows, S. E., Carreras, J., Shaw, N. D. & Humphreys, F. J., 1980.** On mylonites in ductile shear zones. J. Struct. Geol. 2, 175—187.





# RELATIONSHIP BETWEEN ZONAL METAMORPHISM AND DEFORMATION IN THE RANTASALMI—SULKAVA AREA, SOUTHEASTERN FINLAND

by

**Kalevi Korsman and Timo Kilpeläinen**

**Korsman, K. & Kilpeläinen, T. 1986.** Relationship between zonal metamorphism and deformation in the Rantasalmi—Sulkava area, southeastern Finland. *Geological Survey of Finland, Bulletin 339*. 33—42, 12 figures.

Progressive metamorphism in the Rantasalmi—Sulkava area was preceded by a metamorphic phase associated with D1 deformation. Although marked metamorphic facies discordances are lacking in the areas of progressive metamorphism and the grade of metamorphism increases towards the thermal dome at Sulkava, the development of progressive metamorphism can be divided into different stages in relation to the deformation phases. The decomposition reaction of muscovite and the associated crystallization of potassium feldspar and sillimanite took place during the second deformation phase as did the growth of andalusite porphyroblasts in the less metamorphosed portion of the area. The crystallization of cordierite accompanying the decomposition of biotite occurred during D3 deformation, but garnet and cordierite did not attain equilibrium until after the D3 deformation.

Key words: metamorphism, deformation, minerals, crystallization, metapelite, Proterozoic, Rantasalmi, Sulkava, Finland.

*Geological Survey of Finland, SF-02150 ESPOO, Finland*

## INTRODUCTION

The present study delineates the relationship of deformation to progressive metamorphism in the Rantasalmi—Sulkava area. The advance of metamorphism in relation to deformation is best studied by establishing the relationship of the growth of the index minerals to the deformation structures (Zwart 1962, Powell 1979 and Bell & Rubenach 1983). It has been pointed out that

progressive metamorphism in the Rantasalmi—Sulkava area resembles metamorphism of the tectonically thickened crust (Korsman *et al.* 1984). If this concept is valid, the age of metamorphism decreases from the least metamorphosed zones of the area towards the most intensely metamorphosed portion. The present study aims to establish the age relations between the metamorphic

zones by means of deformation phases.

Progressive metamorphism has created the following metamorphic zoning in the metapelites of the Rantasalmi—Sulkava area: the andalusite-muscovite zone, the potassium feldspar-sillimanite zone, the potassium feldspar-cordierite zone, the garnet-cordierite-biotite zone and the garnet-cordierite-sillimanite zone (Korsman 1977, Korsman *et al.* 1984). Associated with progressive metamorphism are the reactions given in simplified form below:

1. andalusite → sillimanite
2. muscovite + quartz → potassium feldspar + sillimanite + H<sub>2</sub>O
3. biotite + sillimanite + quartz → potassium feldspar + cordierite + H<sub>2</sub>O
4. biotite + sillimanite + quartz → potassium feldspar + cordierite + garnet + melt
5. cordierite → sillimanite + garnet + quartz

The change in the metamorphic grade is gradual, and on the erosional plane the isograds are regular as the metamorphic grade increases towards the thermal dome at Sulkava (Fig. 1). Only the garnet-cordierite-sillimanite zone at Sulkava is exotic in relation to its environment. In the area of the thermal dome, the crystallization temperature was 750°C and in the environment 670°C. Around the dome the rise in temperature was buffered by reaction 4. The Sulkava thermal dome developed at the closing stage of Proterozoic metamorphism (Korsman *et al.* 1984).

Kalevi Korsman is responsible for overall plan-

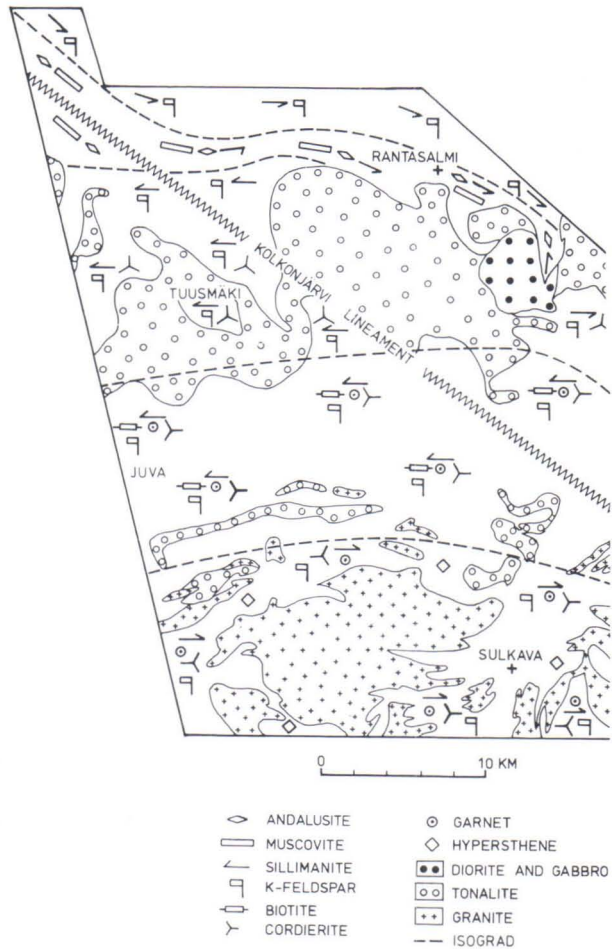


Fig. 1. Metamorphic map of the Rantasalmi—Sulkava area.

ning of the study and Timo Kilpeläinen for establishment of the deformation phases.

### Deformation phases

Four successive deformation phases important in terms of progressive metamorphism can be established in the Rantasalmi—Sulkava metapelite area. Each phase includes folding and various

features related to the axial plane.

The D1 deformation, which deforms the primary structures (S0), manifests itself in the exposures as subisoclinal folding whose axial plane

exhibits shear cleavage (S1, Figs. 2 and 3) caused by fine-grained biotite. S1, however, is generally so weak that it can only be observed under the microscope. S1 has often been almost totally obliterated in metamorphic recrystallization, in which case it may only have survived as inclusions in some porphyroblasts (Fig. 3). Owing to the tightness of F1 folding the cutting angle between S1 and bedding is small.

F2 folding deforms the bedding and the D1 structures (Fig. 2). The F2 folds are isoclinal with a wavelength of several hundreds of metres. The axial planes, F1 and F2, in the outcrops on the flanks of the F2 folds are almost parallel, but at the heads of the F2 folds the cutting relations are clearly visible.

The intensity of S2 schistosity increases with the growth in metamorphic grade. The character of S2 schistosity also depends on the intensity of the S1 to be cut and the cutting angle between S1 and S2. In the northern part of the andalusite-

muscovite zone in particular, S2 exhibits crenulation in S1 at the heads of the F1 folds (discrete crenulation cleavage), but the S2 bands are so tightly packed that the S2 crenulation can only be observed under the microscope (Figs. 2 and 3). In the potassium feldspar-sillimanite zone, S2 is shear cleavage in character and S1 has been almost completely obliterated (Fig. 8).

The D3 that deforms the D1 and D2 structures is seen on the exposures as asymmetric folds of various sizes. In both the andalusite zone and the potassium feldspar-sillimanite zones, S3 is crenulation schistosity that, at its most intense, develops into banding that varies in scale (Figs. 4—6). In the cordierite-potassium feldspar zone, coarse biotite has grown on the S3 plane, resulting in an intense banded structure (Fig. 10).

There does not appear to have been any mineral growth on the axial plane of F4 folding. S4 schistosity is seen as crenulation and folding deforming the older structures (Figs. 4—7).

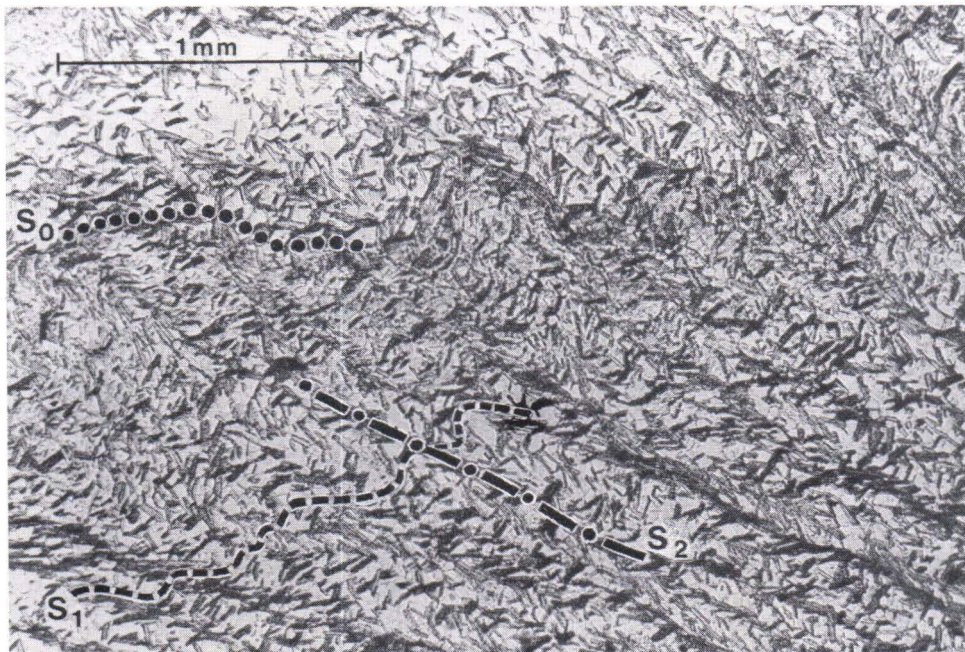


Fig. 2. S1 schistosity subparallel to bedding cut by S2 crenulation — the andalusite zone. Foto by J. Keskinen

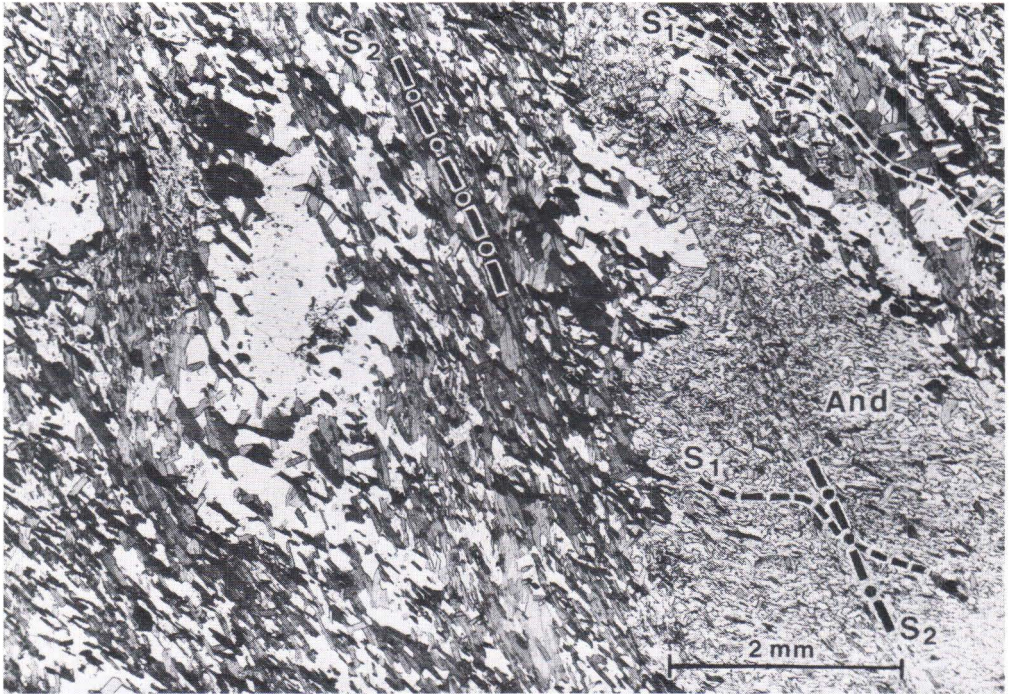


Fig. 3. Andalusite porphyroblasts syntectonic in relation to S2 have overgrown S1 schistosity — the andalusite zone. Foto by J. Keskinen

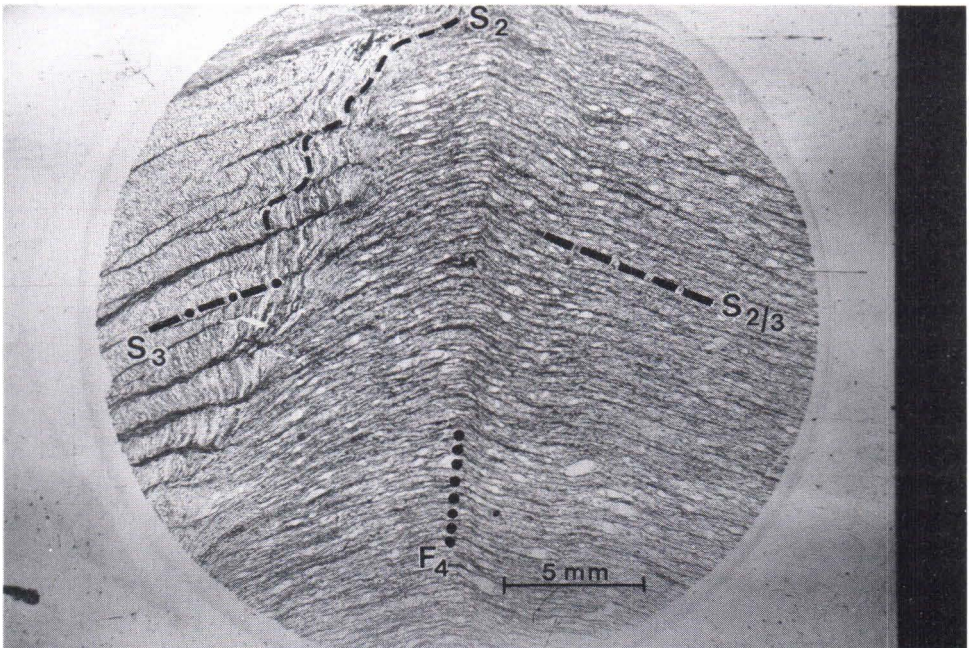


Fig. 4. In psammitic layers S3 is tight-banded, but in pelitic layers the crenulation of S3 is clearly visible — the andalusite zone. Foto by J. Keskinen

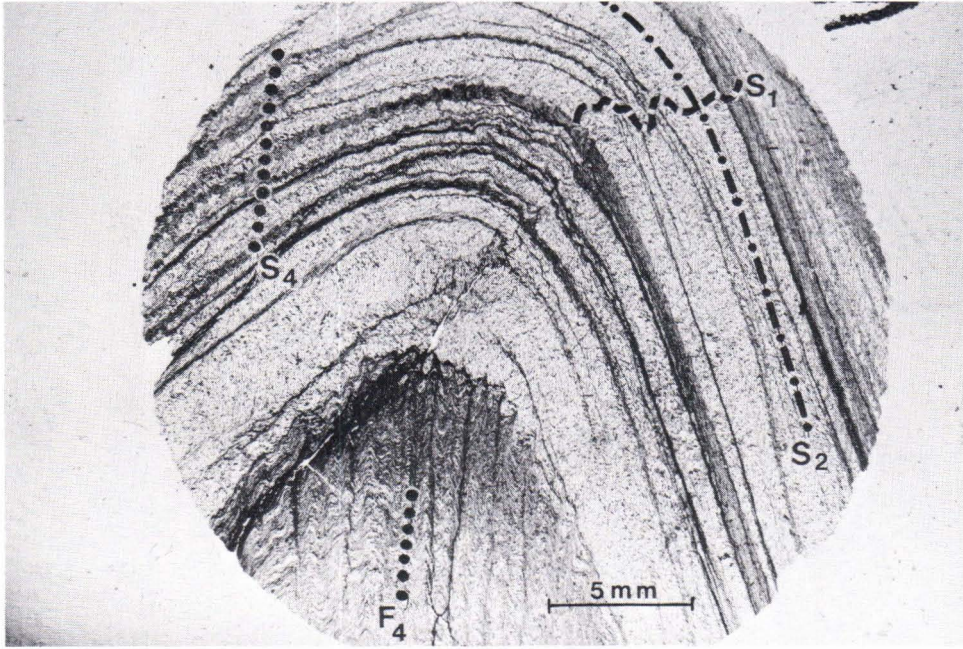


Fig. 5. Banding due to D3 shows folding and crenulation due to D4 — the andalusite zone. Foto by J. Keskinen

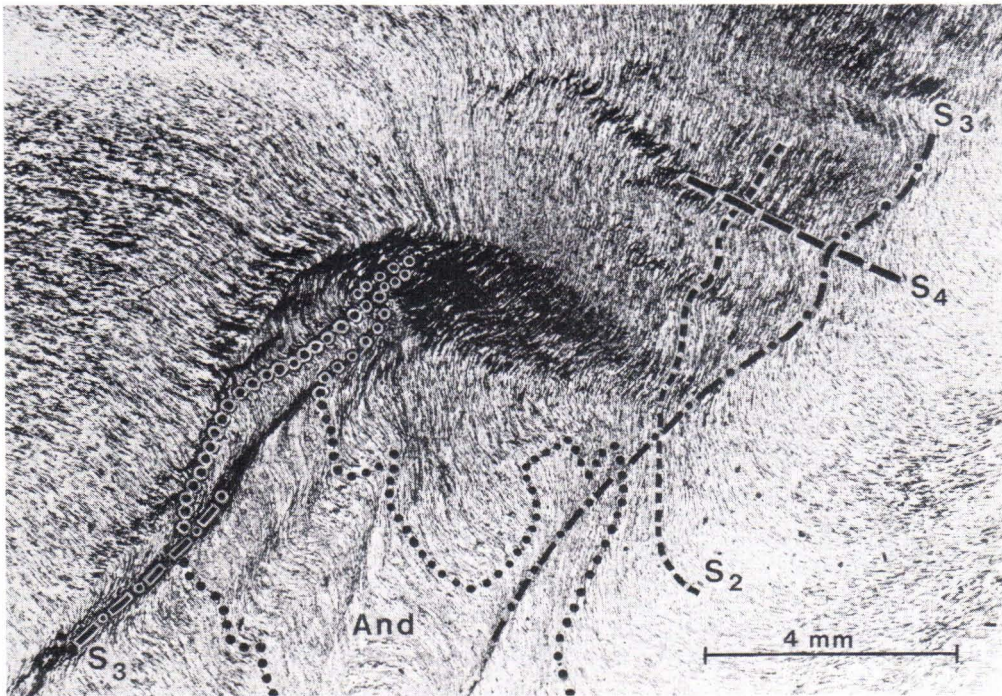


Fig. 6. Andalusite deformed by S3 and S4. Foto by J. Keskinen

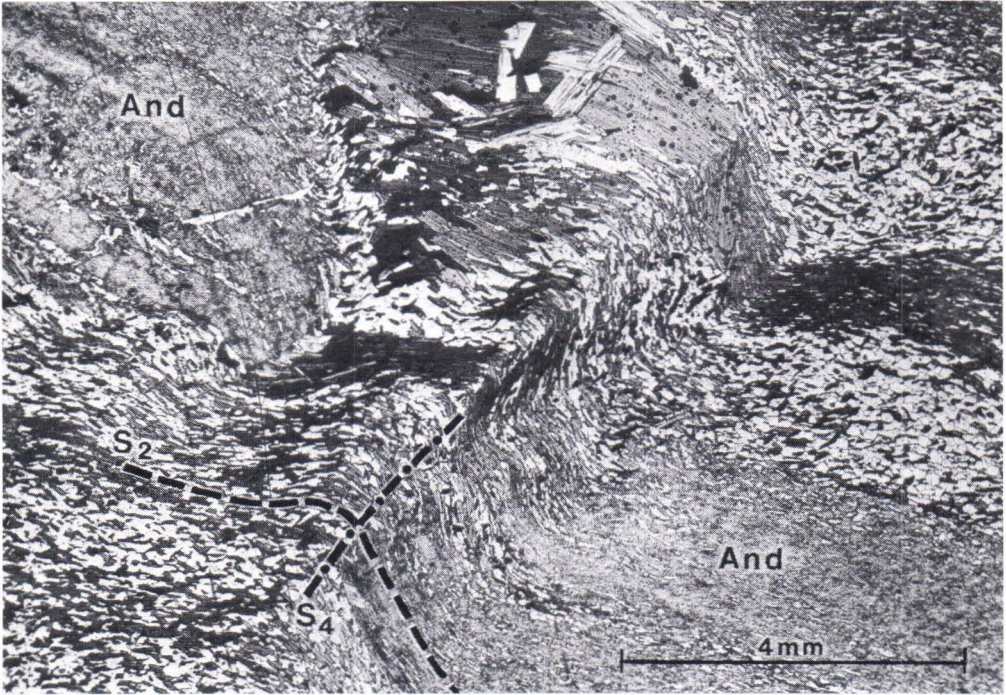


Fig. 7. Optical deformation in an andalusite porphyroblast due to D4. Foto by J. Keskinen

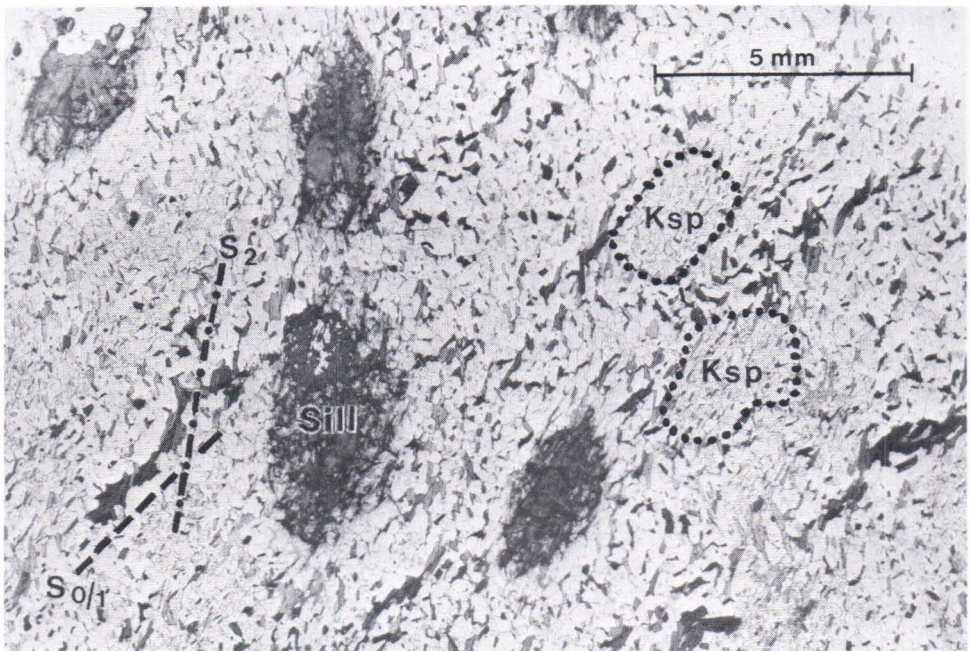


Fig. 8. Potassium feldspar and sillimanite porphyroblasts syntectonic in relation to S2. Foto by J. Keskinen

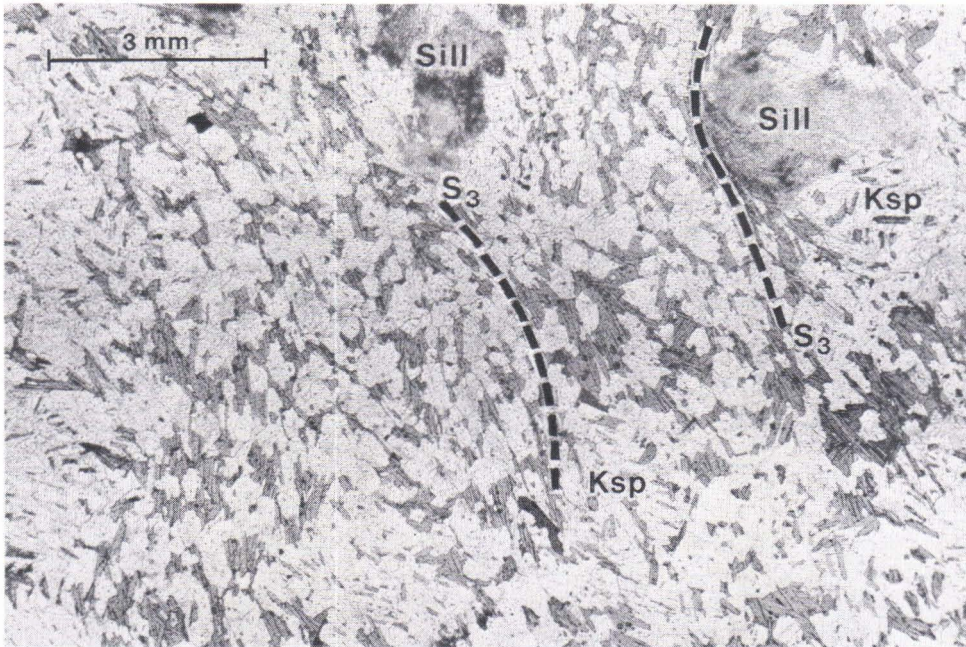


Fig. 9. Sillimanite and potassium feldspar deformed by D3. New biotite has grown on the S3 plane — the potassium feldspar-sillimanite zone. Foto by J. Keskinen

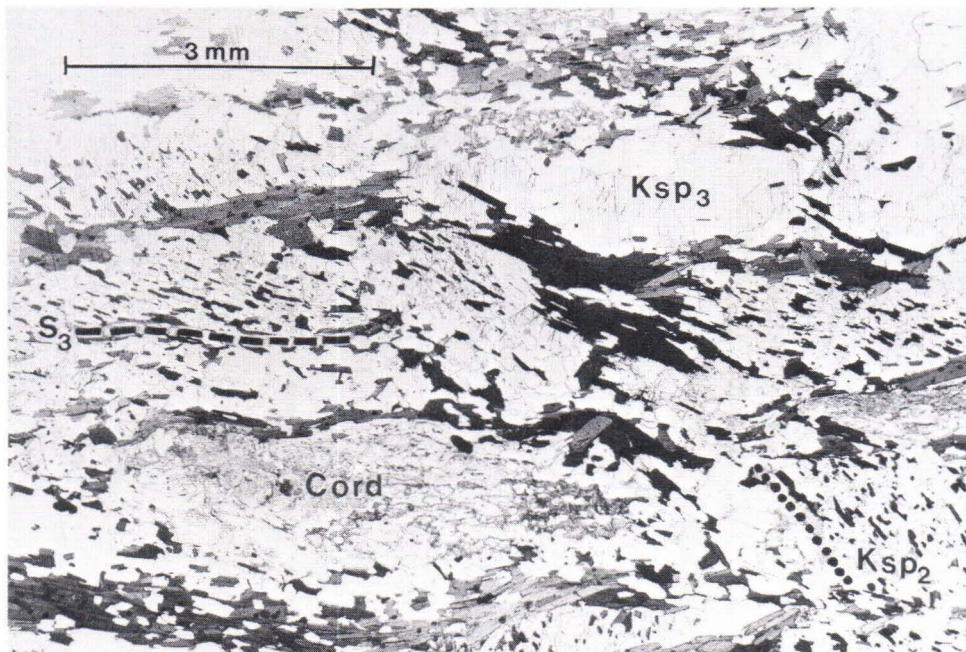


Fig. 10. The early stage of S2 schistosity is visible as a relic in potassium feldspar syntectonic in relation to S2. Cordierite is syntectonic with respect to S3 biotite — the potassium feldspar-cordierite zone. Foto by J. Keskinen



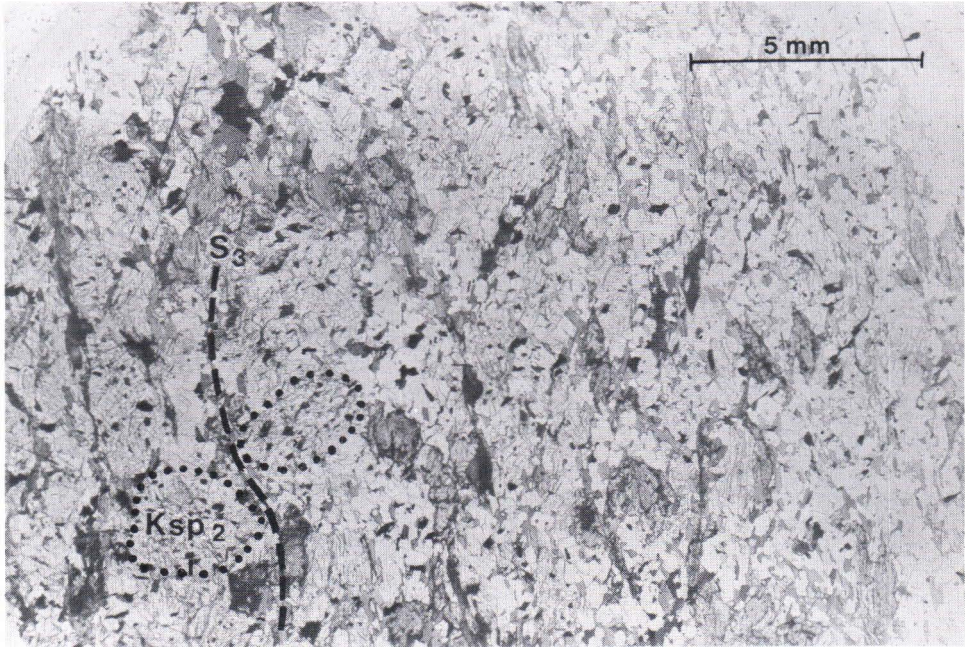


Fig. 11. The predominant schistosity plane in the garnet-cordierite-biotite zone is still S3. S2 has survived as a relic in the Syn-S2 potassium feldspar porphyroblasts. Foto by J. Keskinen

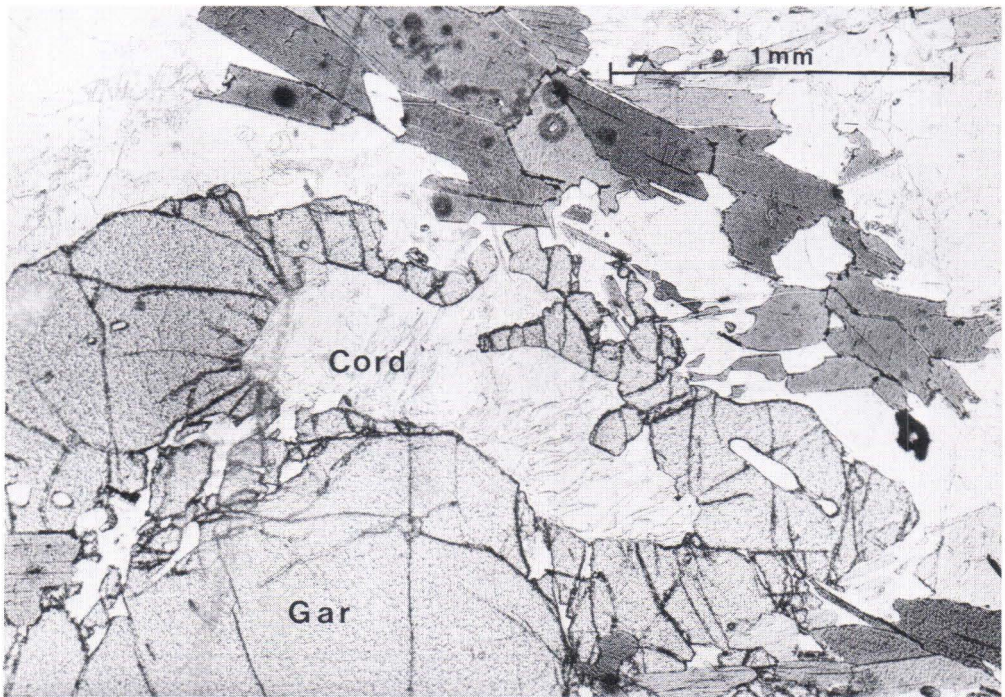


Fig. 12. Garnet and cordierite were equilibrated posttectonically in relation to S3 biotite. Foto by J. Keskinen

### Crystallization of the metamorphic index minerals in relation to deformation

There is no doubt that the andalusite porphyroblasts have overgrown the S1 schistosity (Fig. 3). Andalusite also covers the early stage of S2, as indicated by the weak crenulation of S1 (Fig. 3). The growth of biotite associated with the D2 deformation, however, was simultaneous with that of the andalusite porphyroblasts. The andalusite porphyroblasts are deformed by D3 and D4, which fractured and caused optical deformation in the porphyroblasts (Figs. 6 and 7).

The longitudinal direction of the acicular sillimanite porphyroblasts in the sillimanite-potassium feldspar zone is on the plane of S2 schistosity, but, while growing, sillimanite has replaced S2 biotite (Fig. 8). Sillimanite porphyroblasts are deformed by D3 (Fig. 9). Potassium feldspar porphyroblasts mask the S2 schistosity (Fig. 8). However, the grain size of S2 is distinctly smaller in the inclusions than in the matrix, which means that the grains in the matrix (S2) grow larger after the crystallization of potassium feldspar. The above observations on the crystallization of sillimanite and potassium feldspar in relation to the S2 schistosity show that both phases crystallized simultaneously.

In the potassium sillimanite zone, but particu-

larly in the potassium feldspar-cordierite zone, S3 biotite masks the S2 schistosity in the matrix. S2 has often survived only as inclusions in potassium feldspar that is syntectonic in relation to S2 (Figs. 9—11). The orientation of the S2 inclusions in the potassium feldspar is similar in all porphyroblasts, demonstrating that the potassium feldspars did not rotate during D3 deformation (Bell 1985). Wherever the D3 deformation is well-developed, the exposures show, in addition to bedding, intense banded cleavage due to S3 biotite. The cordierite porphyroblasts and potassium feldspar porphyroblasts formed in the decomposition reaction of biotite (reaction 3) are syntectonic with respect to S3 (Figs. 10 and 11).

The garnet and cordierite equilibrated (reactions 4 and 5) mainly after the D3 deformation (Fig. 12). No observations have been made on the relation of reactions 4 and 5 to D4. In the area of the Sulkava thermal dome, garnet has occasionally been compressed very strongly parallel to the schistosity. It has not, however, been possible to correlate the schistosity to deformation phases established outside the Sulkava thermal dome.

### Discussion

Progressive metamorphism in the Rantasalmi—Sulkava area was preceded by a weak metamorphic event in association with D1 deformation.

Although in the areas of progressive metamorphism the metamorphic grade changes gradually up to the Sulkava thermal dome — no significant metamorphic facies discordances having been noted — the progressive metamorphism can be divided into stages that differ from each other in terms of deformation phases.

The decomposition reaction of muscovite (reaction 2) and the associated crystallization of potassium feldspar and sillimanite occurred during D2 as did the growth of the andalusite porphyroblasts. The relations of the growth of andalusite, potassium feldspar and sillimanite to the coarse S2 biotite (Figs. 3 and 8) indicate that the decomposition reaction of muscovite took place at a later stage of D2 than did the crystallization of andalusite.

The first decomposition reaction of biotite

(reaction 3) with the accompanying crystallization of potassium feldspar and cordierite took place during the D3 stage. Cordierite overgrew the D2 sillimanite, and the D2 potassium feldspar porphyroblasts containing S2 inclusions survived as relics up to the Sulkava thermal dome (Figs. 9—11 and Korsman *et al.* 1984). This implies that the potassium feldspar-cordierite gneisses and the garnet-cordierite-biotite gneisses were primarily sillimanite-potassium feldspar gneisses; it may also imply that there was a time lag between reactions 2 and 3. On account of intense melting, the D2 potassium feldspars have disappeared from the area of the Sulkava thermal dome.

Garnet and cordierite equilibrated in the metapelites (reactions 4 and 5) after the D3 stage (Fig. 12). In the Rantasalmi—Sulkava area, this equilibration was a complex event, as shown by the buffering of the temperature in the garnet-cor-

dierite-biotite zone. Nevertheless, all observations indicate that reaction 5 took place after the D3 stage.

The observation on the relationship of the advance of progressive metamorphism to deformation indicates that the age of metamorphism decreases towards the Sulkava thermal dome. This is compatible with the metamorphism of a tectonically thickened crust. However, it is not easy to attribute the intense rise in temperature merely to the tectonically thickened crust in the area of the Sulkava thermal dome (Korsman *et al.* 1984, p. 37). The relationship of progressive metamorphism to deformation also indicates the complexity of the metamorphic evolution. Because it has not been possible to link the equilibration of garnet and cordierite to the deformation phases, we do not know in which direction the reactions, as a function of time, advanced with respect to the Sulkava thermal dome.

### Acknowledgements

We wish to express our thanks to Mr. Pekka Wasenius who gave us help at various stages of

this study. This manuscript was translated into English by Mrs. Gillian Häkli.

### REFERENCES

- Bell, T. H., 1985.** Deformation partitioning and porphyroblast rotation in metamorphic rocks: a radical reinterpretation. *J. metam. geol.* 3, (2), 109—118.
- Bell, T. H. & Rubenach, M. J., 1983.** Sequential porphyroblast growth and greenschist cleavage development during progressive deformation. *Tectonophysics* 92, 171—194.
- Korsman, K., 1977.** Progressive metamorphism of the metapelites in the Rantasalmi—Sulkava area, southeastern Finland. *Geol. Surv. Finland, Bull.* 290, 82 p.
- Korsman, K., Hautala, T., Hölttä, P. and Wasenius, P., 1984.** Metamorphism as an indicator of evolution and structure of the crust in Eastern Finland. *Geol. Surv. Finland, Bull.* 328, 40 p.
- Powell, C. McA., 1979.** A morphological classification of rock cleavage. *Tectonophysics* 58, 21—34.
- Zwart, H. J., 1962.** On the determination of polymetamorphic mineral associations, and its application to the Bosost area (Central Pyrenees). *Geol. Rundschau* 52, 38—65.

# OBSERVATIONS ON THE METAMORPHIC REACTIONS AND PT CONDITIONS IN THE TURKU GRANULITE AREA

by  
**Pentti Hölttä**

**Hölttä, P., 1986.** Observations on the metamorphic reactions and PT conditions in the Turku granulite area. *Geological Survey of Finland, Bulletin 339*. 43—58, pages, 7 figures, 13 tables.

The Turku area is one of the granulite areas in the migmatite belt of southern Finland, which are characterized by high T, low P and an intensity maximum attained at a rather late stage of metamorphism. Samples taken from the garnet-cordierite gneiss at Lemu and Mietoinen, north of Turku, and from the potassium granite migmatizing it suggest that at the culmination of metamorphism the temperature was c. 800°C and the pressure 5—6 kilobars. Owing to a deficiency of sillimanite, however, the decomposition reaction of biotite has not proceeded to the very end in metapelites. The rocks have undergone very intense retrograde metamorphism, which is seen as zoning in garnet and as crystallization of andalusite and biotite during the retrogressive stage. The cores of the large garnet grains, which are over 5 mm in diameter, contain 25 % pyrope, whereas the smaller grains have a pyrope content of 15—18 %.

Key words: granulites, granites, gneisses, chemical composition, mineral composition, metamorphism, P-T conditions, Proterozoic, Lemu, Mietoinen, Finland.

*Geological Survey of Finland, SF-02150 ESPOO, Finland*

## INTRODUCTION

Rocks of the granulite facies in the migmatite belt of southern Finland have been described from the Turku area (Hietanen 1943, 1947), western Uusimaa (Parras 1958, Schreurs 1984, 1985 a, b, Westra and Schreurs 1985, Schreurs and Westra 1986) and the Sulkava area (Korsman 1977) (Fig. 1). Low-pressure metamorphism is a

feature common to them all; PT determinations indicate that the metamorphic pressure hardly ever exceeded 5 kilobars. The metamorphism in the granulite areas of southern Finland is relatively young. The U-Pb ages of zircon from the palaeosome and neosome of the migmatite in the thermal dome at Sulkava show that metamor-

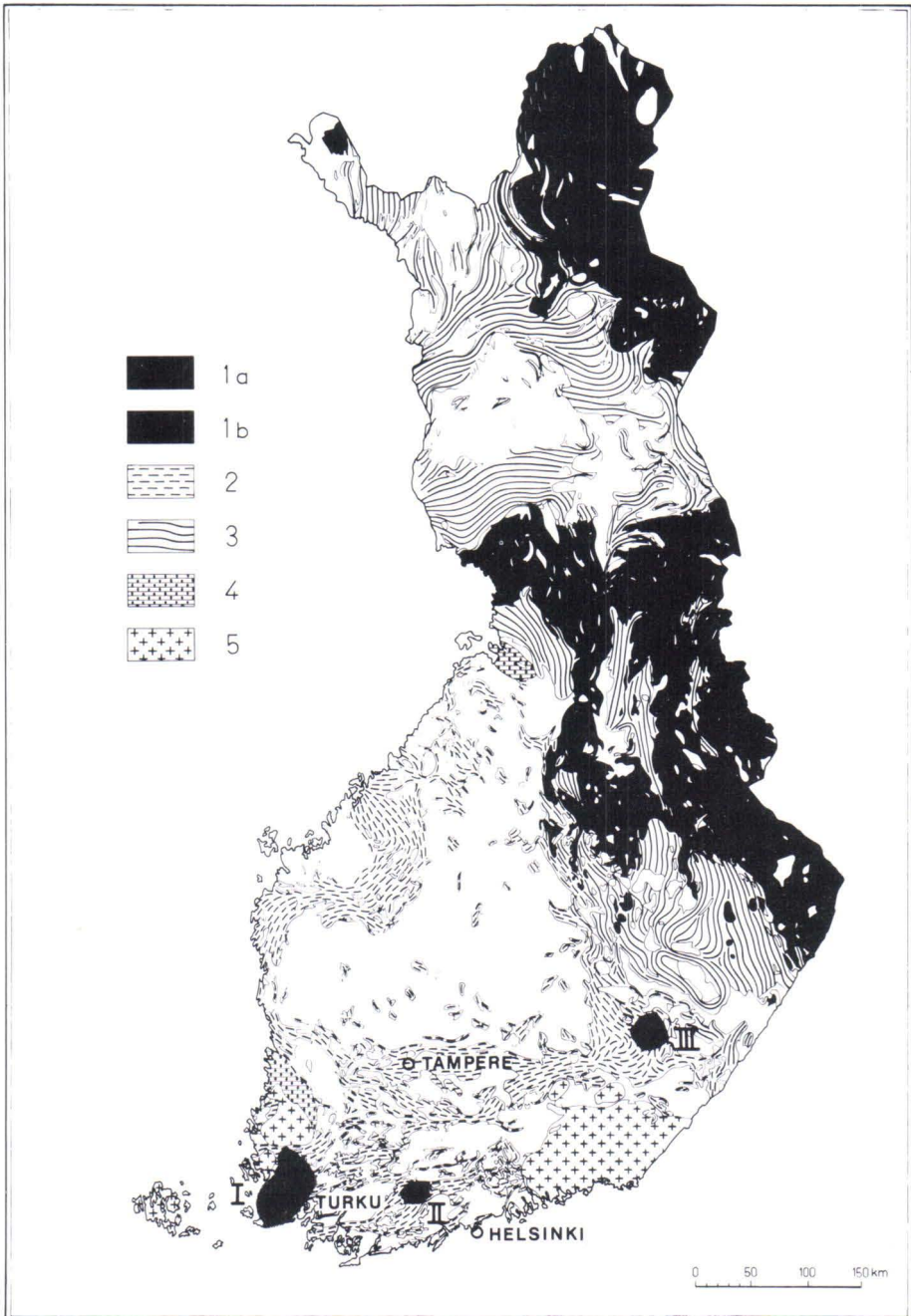


Fig. 1. General geological map of Finland (Simonen 1980). The stippled parts indicate the known granulite areas of the migmatite belt of southern Finland. I = the Turku area (Hietanen 1943, 1947); II = western Uusimaa (Parras 1958, Schreurs 1985 a, b, Westra and Schreurs 1985); III = Sulkava (Korsman 1977). 1a = Archaean complex; 1b = the Lapland granulite area; 2 = the Svecofennidic schist belt; 3 = the Karelian schist belt; 4 = Jotnian sediments; 5 = rapakivi granites.

phism culminated between 1830 and 1810 Ma B.P. (Korsman *et al.* 1984).

The present study seeks to clarify the crystallization history and the PT conditions of the pelitic rocks in the Turku granulite area. Most of the supracrustal rocks in the Turku area are high-grade migmatitic mica gneisses characterized by a great abundance of anatectic granite. Hietanen (1943, 1947) divided the plutonic rocks in the area into an older charnockite and trondhjemite series, younger potassium granites, and posttectonic intrusions that are mainly rapakivi granites (see also Vormo 1976, Vaasjoki 1977). The general geological features of the area are depicted in Fig. 2. Samples were taken from two outcrops in the municipalities of Lemu and Mietoinen, north of Turku. The first outcrop is a road cutting in the village of Kaitainen, Lemu (map sheet 1044 04,  $x=6719.74$ ,  $y=553.66$ ), in which the rock is potassium granite; there are also garnet-cordierite gneiss exposures in the environment. The second outcrop is in the Mietoinen municipal centre (map sheet 1044 05,  $x=6724.32$ ,  $y=551.18$ ), where the potassium granite and garnet-cordierite gneiss are in contact with each other.

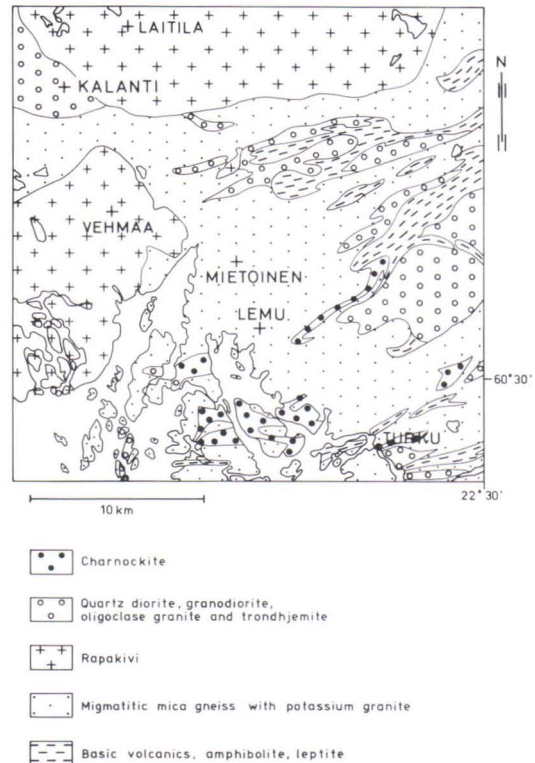


Fig. 2. General geological map of the Turku area; simplified after Härme (1958) and Hietanen (1947).

## METHODS

Twenty-five samples were collected from the garnet-cordierite gneisses and granites, and polished thin sections were cut from them. The petrography of the rocks was studied under an optical microscope. The mineral analyses were performed on a JEOL-JCXA microanalyser at the Institute of Electron Optics of the University of Oulu using the ZAF correction program. The analytical procedure was largely the same as that described by Alapieti and Sivonen (1983). The

whole-rock analyses were done at the Geochemistry Department of the Geological Survey of Finland using the XRF method. The triclinicity of the feldspar was determined by the XRD technique from eight granite and two garnet-cordierite gneiss samples. The modal composition of the garnet-cordierite gneisses was established by point counter analysis, 1000 points being counted on each polished thin section.

## GRANITE

The granite in the present study is considered as the neosome of the garnet-cordierite gneiss,

which occurs as veins from less than 1 cm to several tens of metres wide. In some places the

Table 1. Chemical analyses of granite.

	M-A	M-B	M-C	M-G	L-A	L-D
SiO <sub>2</sub>	74.33	75.01	75.19	72.52	75.54	76.98
TiO <sub>2</sub>	0.07	0.06	0.07	0.05	0.17	0.13
Al <sub>2</sub> O <sub>3</sub>	13.97	14.00	14.12	14.83	13.77	14.43
FeO (tot.)	0.56	0.31	0.34	1.27	0.28	0.86
MnO	0.00	0.00	0.00	0.00	0.00	0.00
MgO	0.28	0.35	0.31	0.99	0.23	0.46
CaO	0.56	1.12	0.69	1.28	1.49	1.01
Na <sub>2</sub> O	2.01	2.92	2.26	2.61	2.38	1.67
K <sub>2</sub> O	7.61	5.21	7.67	3.70	5.32	3.68
P <sub>2</sub> O <sub>5</sub>	0.20	0.20	0.22	0.15	0.15	0.15
Rb	0.025	0.017	0.029	0.015	0.009	0.00
Sr	0.015	0.015	0.017	0.015	0.015	0.00
Zr	0.01	0.00	0.007	0.00	0.00	0.00
Ba	0.08	0.06	0.08	0.05	0.05	0.02
tot.	99.71	99.28	101.02	97.48	99.40	99.38

Samples M-G and L-D contain AFM minerals as porphyroblasts.

Table 2. Chemical analyses of garnet-cordierite gneisses.

	M-1	L-2
SiO <sub>2</sub>	68.51	57.45
TiO	0.77	0.87
Al <sub>2</sub> O <sub>3</sub>	14.43	20.01
FeO (tot.)	6.44	9.25
MnO	0.06	0.11
MgO	2.82	3.51
CaO	1.97	1.12
Na <sub>2</sub> O	2.27	1.56
K <sub>2</sub> O	2.01	4.81
P <sub>2</sub> O <sub>5</sub>	0.13	0.12
Rb	0.016	0.02
Sr	0.021	0.017
Zr	0.012	0.006
Ba	0.05	0.10
tot.	99.52	98.96

Sample L-2 contains sillimanite and potassium feldspar; sample M-1 does not.

veins cut the structures of the gneiss, but in general they are conformable, following, for instance, the shapes of the folds. As a rule the widest veins are coarse grained and often exhibit pegmatitic portions. Euhedral garnet up to 20 mm across is typical of the granite, which also often contains euhedral cordierite as blebs, bands or horizons. According to the classification of

Table 3. Modal compositions of garnet-cordierite gneisses.

	1.	2.
Quartz	31.2	22.1
Plagioclase	30.5	13.1
K-feldspar	0.2	20.3
Garnet	3.6	7.9
Cordierite	11.4	16.0
Biotite	22.1	17.0
Sillimanite	0.0	1.1
Andalusite	0.2	0.8
Accessories	0.5	1.5

The compositions are averages of three determinations. Composition 1 represents analysis M-1 in Table 2 and composition 2 represents analysis L-2.

Streckeisen and LeMaitre (1979), the rocks are alkali granites, monzogranites and syenogranites (Table 1).

The mineral assemblage consists of potassium feldspar, quartz, plagioclase, cordierite, garnet, sillimanite, andalusite, biotite, sericite, carbonate, chlorite, zircon and ilmenite. In the classification of White and Chappell (1983), the rocks are S-type granites in mineralogy and chemistry ( $Al_2O_3/CaO + K_2O + Na_2O > 1.05$ ). According to Härme (1965), the palaeosome of the migma-

tites is, however, often too poor in potassium to give rise to an in-situ potassium-rich granite. On the other hand, Kays (1976) has demonstrated

that the intensely migmatized portions of the gneiss are richer in potassium and poorer in calcium than are the portions that lack veining.

### Petrography and mineral chemistry

As shown by the XRD studies, the potassium feldspar is almost exclusively orthoclase. It occurs as large grains that average 5–15 mm in size but may measure up to several centimetres. The mineral contains abundant perthite and has altered along the fractures into sericite and carbonate. In places, the potassium feldspar exhibits graphic texture.

The grain size of the plagioclase varies from 2 to 10 mm. The mineral often shows normal zoning and sericitization along the fractures. Occasionally antiperthite is encountered. A plagioclase grain in contact with garnet was assayed on

a microanalyser, showing its composition to be  $X_{An} = 0.24$  (Table 7).

Cordierite occurs most often as rectangular grains 2 to 10 mm in size. Along the boundaries and fractures it has invariably altered into fine-grained muscovite, chlorite and green biotite and often into andalusite as well. Some cordierite grains are completely pinitized and a few grains exhibit abundant acicular sillimanite inclusions (Fig. 3). Small quartz inclusions are rare and often altogether absent. In the garnetiferous portions cordierite and garnet are frequently in contact with each other. The cordierite in contact

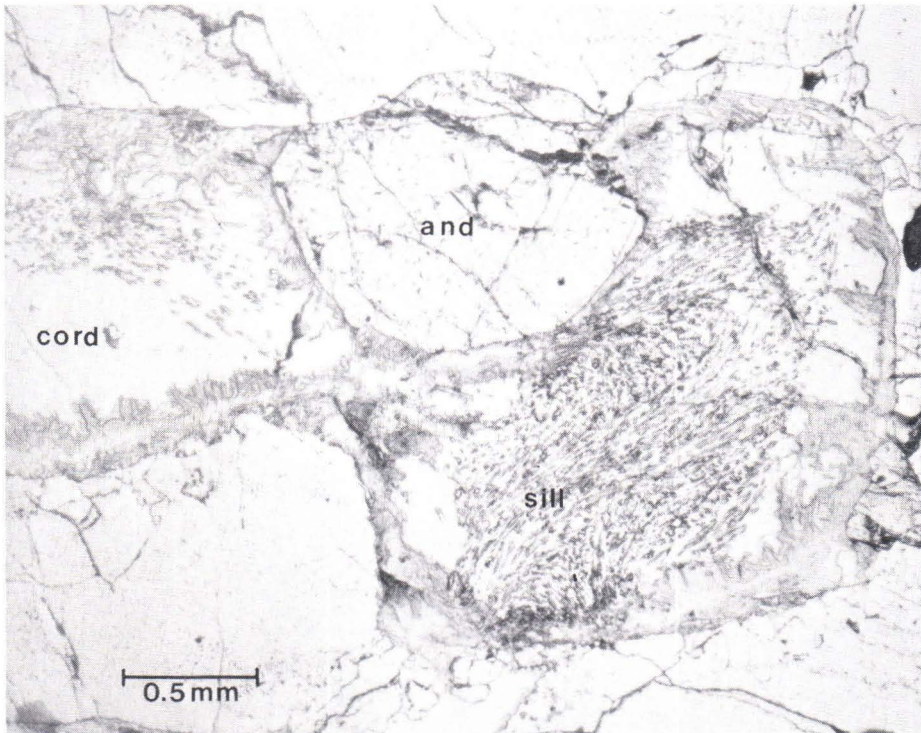


Fig. 3. A cordierite grain in granite pinitized along the edges and having andalusite and sillimanite as retrograde alteration products.



Table 4. Microprobe analyses of garnets in granite.

Grain diameter	L-3-33 1.5 mm		L-4 1 mm		M-4-9 10 mm		M-E-6 2 mm		M-A-20 0.5 mm
	core	edge	core	edge	core	edge	core	edge	core
	SiO <sub>2</sub>	37.86	37.28	37.68	37.69	38.93	38.58	38.12	38.22
TiO <sub>2</sub>	—	—	—	—	—	—	—	—	—
Al <sub>2</sub> O <sub>3</sub>	21.30	21.33	21.67	21.48	22.21	21.94	21.57	21.63	21.75
FeO (tot.)	35.06	36.73	35.56	36.88	32.28	35.20	34.43	35.30	35.50
MnO	0.59	0.77	0.55	0.75	0.46	0.62	0.65	0.63	0.70
MgO	3.83	2.57	3.30	2.47	6.44	4.28	4.41	3.86	3.68
CaO	0.77	0.71	0.77	0.72	0.81	0.78	0.72	0.67	0.72
Na <sub>2</sub> O	—	—	—	—	—	—	—	—	—
K <sub>2</sub> O	—	—	—	—	—	—	—	—	—
Tot.	99.41	99.39	99.53	99.99	101.13	101.40	99.90	100.31	100.41

Table 5. Microprobe analyses of cordierites in granite.

	M-4-9	M-E-6	L-6
SiO <sub>2</sub>	50.22	48.85	48.69
TiO <sub>2</sub>	—	—	—
Al <sub>2</sub> O <sub>3</sub>	33.61	32.76	32.76
FeO (tot.)	7.70	8.52	8.87
MnO	0.06	0.06	0.03
MgO	8.72	7.95	7.67
CaO	—	—	—
Na <sub>2</sub> O	0.10	0.18	0.17
K <sub>2</sub> O	—	—	—
tot.	100.41	98.32	98.19

L-6 is a single euhedral crystal surrounded by feldspars and quartz.

with garnet is richer in Mg than is the single euhedral cordierite. Table 5 lists the chemical compositions of some cordierites.

The garnet grains vary from about 0.5 mm to 20–30 mm in size. In the large grains, up to half of the volume may be occupied by quartz inclusions, and the grains are often surrounded by quartz. Along the edges and fractures, the garnet has altered into green biotite and is occasionally surrounded by a narrow cordierite rim. Some grains contain not only quartz but also abundant acicular sillimanite as inclusions. The garnet is intensely zoned,  $X_{Mg}$  decreasing clearly and  $X_{Fe}$ ,  $X_{Ca}$  and  $X_{Mn}$  increasing slightly from the core of the grain towards the rim (Table 4). In the core of the large grains (diameter > 5 mm),  $X_{Mg}$  is

Table 6. Microprobe analyses of biotites in granite.

	L-3-33	M-A-20	M-C
SiO <sub>2</sub>	34.91	36.14	35.86
TiO <sub>2</sub>	0.04	0.06	2.83
Al <sub>2</sub> O <sub>3</sub>	20.46	19.90	19.48
FeO (tot.)	17.96	18.75	20.39
MnO	0.00	0.04	0.06
MgO	10.82	10.85	8.33
CaO	0.13	0.11	0.04
Na <sub>2</sub> O	0.15	0.16	0.11
K <sub>2</sub> O	8.37	8.52	8.81
tot.	92.84	94.53	95.91

M-C is a large single reddish brown biotite, M-A-20 and L-3-33 are green biotites that are alteration products of garnet.

Table 7. An analysis of plagioclase in granite.

	L-4
SiO <sub>2</sub>	61.81
TiO <sub>2</sub>	—
Al <sub>2</sub> O <sub>3</sub>	23.73
FeO (tot.)	0.11
MnO	—
MgO	—
CaO	5.06
Na <sub>2</sub> O	8.98
K <sub>2</sub> O	0.14
tot.	99.80

0.25. The smaller grains are distinctly poorer in Mg and their  $X_{Mg}$  averages 0.15, which could possibly be attributed to the fact that the cores

of the larger grains have retained the composition corresponding to the culmination of metamorphism whereas the smaller grains have undergone retrograde re-equilibration.

There are two generations of biotite. The older one is reddish brown and averages 0.05–2 mm in size. The younger, retrograde biotite occurs as c. 0.1–0.3 mm long flakes, which are generally pale green but occasionally brown and alteration products of cordierite and garnet. The green biotite is rather poor in Ti ( $\text{TiO}_2 = 0.04\text{--}0.6\%$ ) and contains appreciable Ca ( $\text{CaO} = 0.11\text{--}0.13\%$ ) (Table 6) because it derives from garnet

(cf. Gorbatshev 1972, Brown and Phadke 1983, Tracy and Dietsch 1982).

Sillimanite occurs in cordierite as 0.1–1 mm long prisms or thin acicular inclusions, 0.05–0.5 mm in length. The larger grains generally border the potassium feldspar crystals or constitute inclusions in them.

Andalusite is a product of the retrograde decomposition of cordierite (Fig. 3). As a rule it occurs as euhedral grains, 0.1–1 mm in size, or as anhedral intergrowths with the green biotite at the borders of the cordierite grains. The mineral is normally free from inclusions.

### GARNET-CORDIERITE GNEISS

The garnet-cordierite gneiss is intensely recrystallized, and primary structures are rare. Occasionally the rock exhibits fine-grained bands that are more acidic than the environment and probably indicate bedding. The rock is granoblastic in texture.

The mineral assemblages depend on the chemical composition of the rock and are either

- 1) gar-cord-bio-and-pl-qz-ilm-magn-graph  
or
- 2) gar-cord-sill-bio-ksp-pl-qz-ilm-magn-graph.

Assemblage 2 occurs in portions of the gneiss

that are richer in Al and K than the portions with assemblage 1 (Table 2). The  $\text{K}_2\text{O}$  content approaches five per cent and is thus not much lower than that in granite. The chemical composition does not contradict the possibility that the granitic melts were formed in situ (cf. Korsman 1977).

Like the granite, the garnet-cordierite gneiss exhibits features of intense retrograde metamorphism manifested by reactions that often result in the crystallization of andalusite.

Modal compositions of the garnet-cordierite gneiss are given in Table 3.

### Petrography and mineral chemistry

Potassium feldspar is mainly orthoclase as shown by the XRD identification and has an average grain size of 0.5–2 mm. It contains micropertthite exsolution bodies, is slightly sericitized along the rims and fractures, and often contains quartz and biotite inclusions. Table 12 lists the chemical compositions of some potassium feldspars.

Plagioclase varies from 0.1 to 1.5 mm. Its is

slightly sericitized along the fractures and contains exsolved antiperthite and biotite inclusions. Occasionally sillimanite inclusions are also present, and weakly developed normal zoning occurs here and there. The composition of the mineral is  $X_{\text{An}} = \text{c. } 0.25$  (Table 11).

Cordierite occurs both as rectangular grains, 1–5 mm in size, and as alteration products of garnet (Fig. 4), in which case the grains are the

same shape as the earlier garnet. Occasionally the grains are elongated along the schistosity and may be up to 10 mm in length. The cordierite contains biotite, quartz and sillimanite as inclusions, the latter being almost invariably in the middle of the cordierite grains, their longitudinal axis parallel to that of the host mineral. The cordierite is often pinitized along the fractures although not as intensely as in the granite. The rims of the grains have undergone retrograde alteration into biotite, andalusite and sillimanite. The cordierite that is in contact with garnet is somewhat richer in Mg than is the cordierite in the matrix (Table 9).

Garnet occurs as poikiloblasts, 1–10 mm in size, with abundant quartz and biotite and sometimes also sillimanite as inclusions. The mineral has frequently altered into cordierite along the rims. (Fig. 4) The edges and fractures are rimmed with a narrow (c. 0.01 mm) pale green biotite seam. However, the biotitization is not nearly

as intense as it is in the granite. The core of the large grains is very rich in Mg as it is in the granite ( $X_{Mg}=0.25$ ); in the smaller grains the pyrope content is lower ( $X_{Mg}=0.18$ ). The value of  $X_{Mg}$  decreases markedly and that of  $X_{Mn}$  increases slightly from the cores of the grains towards the edges (Table 8).

Biotite has at least two generations. The older biotite is reddish brown and averages 0.2–0.5 mm in grain size. The biotite that occurs as inclusions in garnet, cordierite and potassium feldspar is smaller, averaging 0.1–0.2 mm in diameter. The inclusion biotite grains are presumably prograde relics, but the biotite in the matrix continued to grow after the crystallization of garnet and cordierite. Occasionally the cordierite grains are also rimmed with the younger pale green retrograde biotite that occurs as fine-grained flakes (< 0.1 mm). The abundance of green biotite is, however, considerably lower than in the granite, and it is not encountered as an

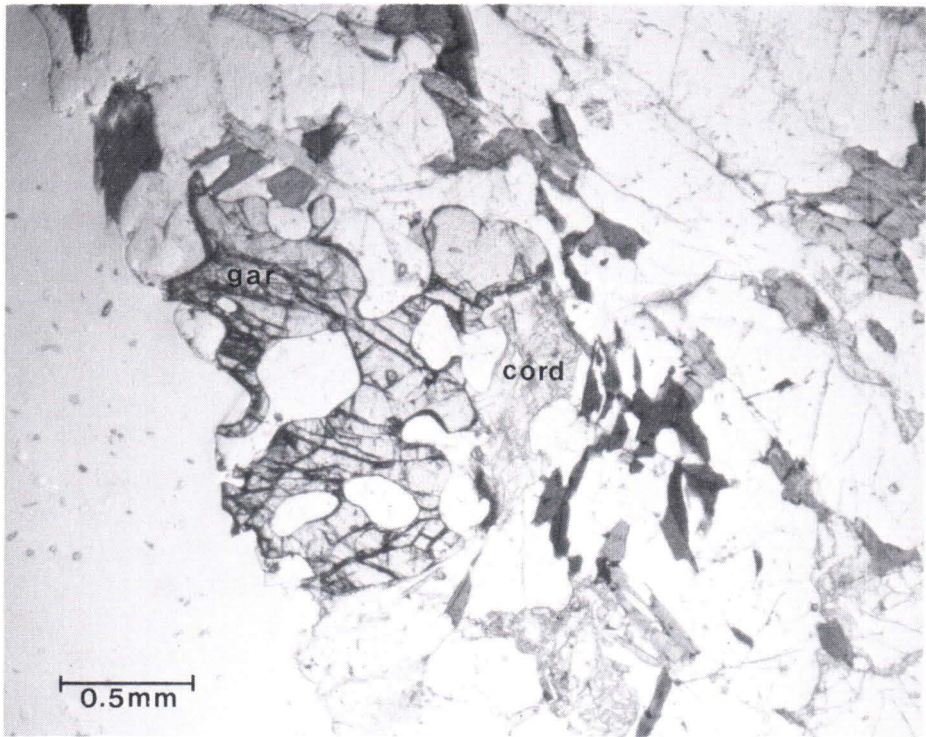


Fig. 4. A garnet grain altered into cordierite along the edges of the grain.

Table 8. Microprobe analyses of garnets in garnet-cordierite gneiss.

Grain diameter	M-5-9 5 mm		M-2-16 1.5 mm		L-1-6 9 mm		L-12 8 mm	L-22 3 mm	L-24 3 mm	M-2-9 1.5 mm	M-2-12 0.5 mm
	core	edge	core	edge	core	edge	core	core	core	core	core
SiO <sub>2</sub>	32.29	38.26	38.21	38.23	39.04	38.48	38.93	38.38	38.42	37.27	38.52
TiO <sub>2</sub>	—	—	—	—	—	—	—	—	—	—	—
Al <sub>2</sub> O <sub>3</sub>	22.29	21.80	21.64	21.63	21.93	21.87	22.31	21.71	21.68	21.51	21.79
FeO (tot.)	32.82	34.76	34.26	35.28	32.33	36.31	32.48	34.25	34.20	34.11	34.89
MnO	0.59	0.72	0.63	0.80	0.63	0.88	0.63	0.75	0.72	0.70	0.71
MgO	5.66	4.06	4.42	3.77	6.72	3.87	6.00	4.75	4.55	4.59	4.29
CaO	0.82	0.86	0.84	0.84	0.95	0.91	0.93	0.93	0.91	0.83	0.84
Na <sub>2</sub> O	—	—	—	—	—	—	—	—	—	—	—
K <sub>2</sub> O	—	—	—	—	—	—	—	—	—	—	—
tot.	101.47	100.46	100.0	100.55	101.60	102.32	101.28	100.77	100.48	99.01	100.44

Table 9. Microprobe analyses of cordierites in garnet-cordierite gneiss.

	M-5-9	L-1-6	L-22	L-24	M-2-9	M-2-12	M-2-15
SiO <sub>2</sub>	49.53	49.30	47.78	49.04	48.90	49.50	49.49
TiO <sub>2</sub>	—	—	—	—	—	—	—
Al <sub>2</sub> O <sub>3</sub>	33.21	32.81	31.90	33.00	32.93	32.87	32.72
FeO (tot.)	7.81	7.74	7.35	7.58	7.06	8.15	8.48
MnO	0.06	0.06	0.03	0.04	0.03	0.04	0.05
MgO	8.42	8.77	8.12	8.59	8.74	8.22	8.02
CaO	—	—	—	—	—	—	—
Na <sub>2</sub> O	0.10	0.09	0.14	0.08	0.07	0.04	0.11
K <sub>2</sub> O	—	—	—	—	—	—	—
tot.	99.13	98.77	95.32	98.33	91.73	98.82	98.87

M-2-15 is not in contact with garnet.

Table 10. Microprobe analyses of biotites in garnet-cordierite gneiss.

	M-5-9i	M-2-16i	M-2-16	M-2-9	M-2-15	M-5-9m	M-5-9ma	L-1-6m	L-12m
SiO <sub>2</sub>	37.23	36.51	36.40	36.15	36.07	36.62	36.02	36.76	36.96
TiO <sub>2</sub>	2.87	1.97	3.31	3.48	4.07	4.19	4.04	3.95	3.95
Al <sub>2</sub> O <sub>3</sub>	17.33	18.11	18.20	17.37	17.65	17.74	17.29	17.81	17.83
FeO (tot.)	13.70	15.31	17.12	17.13	18.29	18.11	18.23	17.79	17.39
MnO	0.01	0.03	0.02	0.04	0.01	0.00	0.01	0.03	0.00
MgO	14.48	12.96	10.62	11.62	9.94	10.67	10.48	10.86	10.94
CaO	0.00	0.13	0.02	0.02	0.05	0.03	0.00	0.01	0.01
Na <sub>2</sub> O	0.18	0.14	0.10	0.14	0.10	0.09	0.07	0.09	0.10
K <sub>2</sub> O	9.10	8.75	9.39	9.31	9.60	9.27	9.46	9.39	9.57
tot.	94.90	93.91	95.16	95.27	95.78	96.72	95.60	96.69	96.75

Analyses marked with i are from the inclusions in garnet; analyses with m are from matrix biotites. M-5-9m and M-5-9ma are from the same thin section.

alteration product of garnet. Likewise the biotite that was formed at the retrogressive stage, in the reaction between potassium feldspar and cordierite, is usually brown. The biotite in contact with garnet is clearly richer in Mg than is the biotite in contact with cordierite (analysis M-2-15

in Table 10 is of a biotite in contact with cordierite, cf. Korsman 1977, pp 38—39). Richest in Mg is the biotite that occurs as inclusions in garnet; it is also appreciably poorer in TiO<sub>2</sub> than are the biotites in the matrix. The Mg content may be attributed to retrograde re-equilibration (cf. e.g.

Table 11. Microprobe analyses of plagioclases in garnet-cordierite gneiss.

	M-5-9	L-12
SiO <sub>2</sub>	62.88	62.36
TiO <sub>2</sub>	—	—
Al <sub>2</sub> O <sub>3</sub>	23.94	24.26
FeO (tot.)	0.03	0.00
MnO	—	—
MgO	—	—
CaO	4.90	5.22
Na <sub>2</sub> O <sub>3</sub>	8.98	8.92
K <sub>2</sub> O	0.27	0.25
tot.	101.10	101.01

Indares and Martignole 1985b); the same applies to the low TiO<sub>2</sub> (see Korsman 1977, p 41). The TiO<sub>2</sub> content of the inclusions (c. 2 %) is, however, higher than that of the green biotite (TiO<sub>2</sub> < 0.1 %) that occurs in the granite as the alteration product of garnet. This is a strong indication that the biotite inclusions in garnet are older than the garnet; the composition merely changed at the retrogressive stage.

In the potassium feldspar-bearing portions, sillimanite occurs in the cordierite as prisms mea-

Table 12. Microprobe analyses of K-feldspars in garnet-cordierite gneiss.

	M-2-16	L-1-6
SiO <sub>2</sub>	62.45	62.49
TiO <sub>2</sub>	0.02	0.01
Al <sub>2</sub> O <sub>3</sub>	17.99	18.17
FeO (tot.)	0.05	0.00
MnO	—	—
MgO	—	—
CaO	0.09	0.10
Na <sub>2</sub> O	1.39	1.83
K <sub>2</sub> O	14.23	13.73
tot.	96.23	96.33

suring c. 0.05—0.3 mm, and occasionally also in plagioclase. It is further encountered as minute acicular crystals along the edges of the cordierite grains.

Small amounts of andalusite are encountered along the edges of the cordierite grains, where it occurs as tiny grains measuring less than 0.1 mm. It is intergrown with biotite and its abundance is markedly lower than that of the andalusite in granite; it is also much smaller. Andalusite occurs solely as a retrograde phase.

## METAMORPHIC REACTIONS

The chemical and modal compositions of garnet-cordierite gneiss show that the metamorphic reactions were affected by chemistry. In the rocks in which the concentration of aluminium is low in relation to that of alkalis and calcium and in which originally only small amounts of sillimanite crystallized, the abundance of biotite is higher than in sillimanite-bearing rocks. Observations show that in the sillimanite-bearing portions the decomposition reaction of biotites advanced further than in the portions poorer in Al, terminating only when almost all the sillimanite had been consumed.

Examination of thin sections has revealed that the garnet-cordierite gneiss has the following

equilibrated assemblages (assuming that the minerals existing in contact with each other within an area measuring c. 2—3 mm in size are in equilibrium):

car-cord-bio, cord-bio, gar-bio, bio

The portions containing potassium feldspar and sillimanite have the assemblages gar-cord-bio-ksp, cord-bio-ksp, gar-bio-ksp, gar-cord-sill, cord-sill, gar-sill, bio-ksp.

All the assemblages also contain plagioclase and quartz. In addition to them there are the following retrograde assemblages:

cord-bio-sill-and-ksp and gar-bio-ksp.

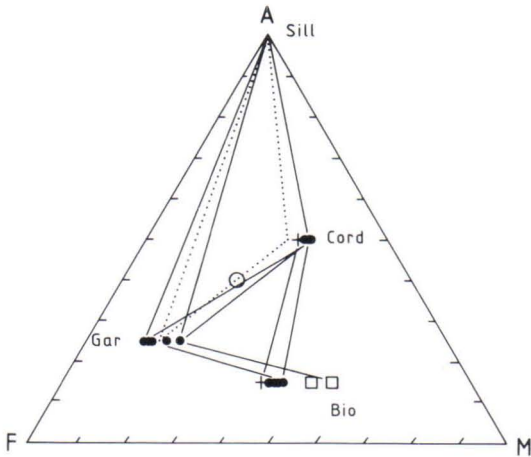


Fig. 5. AFM diagram (potassium feldspar as a projection point) showing the equilibrium mineral assemblages and the compositions of the mineral cores in the garnet-cordierite gneisses. The garnet grades into a more Mg-bearing variant when the grain size increases. The cordierite-biotite assemblage that is not in contact with garnet is marked with a cross. The squares refer to biotite inclusions in large garnet grains. The big circle stands for the total composition of the rock (analysis L-2, Table 2). The stippled triangle shows the compositions of garnet and cordierite in the area of the Sulkava thermal dome (Korsman 1977).

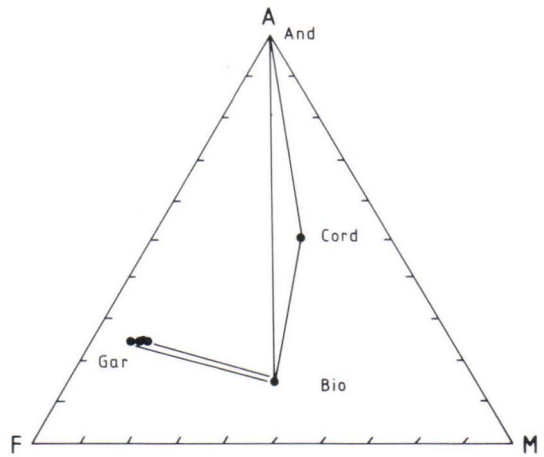


Fig. 6. AFM diagram for the retrograde assemblages of the garnet-cordierite gneisses. The compositions of the garnets measured from the edges of the grains.

The equilibrium mineral assemblages of the garnet-cordierite gneiss are shown on an AFM diagram in Fig. 5 and the retrograde assemblages in Fig. 6.

The observed assemblages demonstrate that at least the following simplified reactions took place in the rock:

1.  $2 \text{ bio} + 6 \text{ sill} + 9 \text{ qtz} = 3 \text{ cord} + \text{ksp} + 2 - 3n \text{ H}_2\text{O}$
2.  $\text{bio} + \text{sill} + 2 \text{ qtz} = \text{gar} + \text{ksp} + \text{H}_2\text{O}$

The assemblage gar-cord-bio-ksp-qtz is less common than any other, possibly owing to the composition of the rock. Sillimanite was almost completely consumed at lower temperatures, and the reaction

3.  $2 \text{ bio} + 8 \text{ sill} + 13 \text{ qtz} = 2 \text{ gar} + 3 \text{ cord} + 4 \text{ ksp} + 4 \text{ H}_2\text{O}$

could not advance very far. The potassium liberated in the decomposition reaction of biotite might have migrated in the form of ions or have entered directly into the melt, because some of the rocks lack potassium feldspar (cf. Thompson 1982).

The gneiss exhibits the retrograde reaction quite clearly, the following reactions, at least, having taken place under the declining PT conditions:

4.  $3 \text{ cord} + \text{ksp} + 2 - 3n \text{ H}_2\text{O} = 2 \text{ bio} + 6 \text{ sill} + \text{and} + \text{qtz}$
5.  $2 \text{ gar} + 4 \text{ sill} + 5 \text{ qtz} + 3n \text{ H}_2\text{O} = 3 \text{ cord}$

Reaction 4 is manifest virtually wherever the cordierite is in contact with potassium feldspar. The reaction also liberated ilmenite and magnetite. The alteration of cordierite and garnet in the granite was of particular intensity but the retrograde reactions of the minerals did not liberate oxides as was the case with the gneisses. In many places garnet has altered into cordierite (Fig. 3, reaction 5), and this process, too, has consumed sillimanite.

## GEOTHERMOMETERS AND GEOBAROMETERS

The established mineral assemblages and the reactions allow the use of geothermometers and geobarometers based on the following assemblages: garnet-biotite, garnet-cordierite-silliman-

Table 13. PT determinations. If not specially mentioned, the analyses refer to the core composition of the minerals. Temperature is in degrees Celsius and pressure in kilobars.

Sample number	Assemblage	T1	T2	T3	P1	P2
L-1-6	9 mm diameter garnet + adjacent cordierite	775			5.1	
M-5-9	5 mm diameter garnet + adjacent cordierite	730			5.2	
L-L-22	3 mm diameter garnet + adjacent cordierite	658			5.4	
L-L-24	3 mm diameter garnet + adjacent cordierite	641			5.5	
M-2-9	1.5 mm diameter garnet + adjacent cordierite	620			5.8	
M-2-12	0.5 mm diameter garnet + adjacent cordierite	651			5.3	
M-2-15	5 mm diameter garnet + matrix cordierite	774			4.8	
M-4-9 (granite)	10 mm diameter garnet + adjacent cordierite	761			5.2	
M-E-6 (granite)	2 mm diameter garnet + adjacent cordierite	684			5.1	
L-1-6m	9 mm diameter garnet + matrix biotite		876	730		
L-12m	8 mm diameter garnet + matrix biotite		791	693		
M-5-9m	5 mm diameter garnet + matrix biotite		803	699		
M-2-16	1.5 mm diameter garnet + adjacent biotite		635	619		
L-3-33 (granite)	garnet rim + adjacent green biotite		448	528		
L-12	8 mm diameter garnet + adjacent plagioclase (T estim. 800 degrees)					6.5
M-5-9	5 mm diameter garnet + adjacent plagioclase (T estim. 800 deg.)					6.3
L-4 (granite)	1 mm diameter garnet + adjacent plagioclase (T estim. 670 deg.)					3.5

T1 = garnet-cordierite temperature according to Holdaway and Lee (1977), T2 = garnet-biotite temperature according to Ferry and Spear (1978), T3 = garnet-biotite temperature according to Perchuk and Lavrentéva (1983), P1 = garnet-cordierite pressure according to Holdaway and Lee (1977) and P2 = garnet-plagioclase pressure according to Newton and Haselton (1981) with  $P^{\circ}(\text{Sill}) = -1.17 + 0.0238T$  (°C) (Ganguly and Saxena 1984, p. 93).

ite-quartz and garnet-plagioclase-sillimanite-quartz. Table 13 lists the temperatures and pressures given by the garnet-biotite thermometer of Ferry and Spear (1976) and Perchuk and Lavrenteva (1983), the garnet-cordierite thermobarometer of Holdaway and Lee (1977) and the garnet-plagioclase barometer of Newton and Haselton (1981). Since the concentrations of Ca and Mn are low in the garnets, the results obtained by using calibrations that take into account the activity of the grossular and spessartite components (Hodges and Spear 1982, Ganguly and Saxena 1984) do not differ much from the results given by the thermometer of Ferry and Spear. In contrast, the temperatures calculated from Per-

chuk and Lavrenteva differ markedly from these at higher temperatures. Perchuk and Lavrenteva (1983, p. 235) themselves point out that the temperatures given by the thermometer for the granulites are probably too low, presumably on account of the Al concentration in biotite.

The partial pressure of water was assumed to be 0.5 when the pressure was calculated from Holdaway and Lee (1977). The abundance of biotite in the garnet-cordierite gneiss is higher than in the Sulkava area (Korsman 1977), which, in addition to the less plentiful sillimanite, may also be attributed to the higher activity of water in the metamorphism.

## DISCUSSION

As shown by the results, the choice of analysis points has a marked effect on the data in an area of intense retrograde metamorphism. The small garnet grains and the biotite and cordierite in contact with them re-equilibrated during the cooling (cf. Perchuk and Lavrenteva 1983, Indares and Martignole 1985 a, b, Schreurs 1985b). Consequently, estimation of the maximum temperatures was based on the compositions of the cores of the large garnet grains and the biotite in the matrix, which was not in contact with the garnet. The method is probably applicable to rocks of the granulite facies provided that high-grade metamorphism has resulted in complete equilibration of Fe and Mg on thin-section scale. The highest temperature thus obtained on the basis of the calibration of Ferry and Spear (almost 900°) is improbable and too high, whereas the other temperatures (around 800°) are realistic considering the general geology of the area. If the PT determinations are based on the compositions of the small garnet grains (which in the thin sections may be marginal parts of large garnets) and those of the biotites and cordierites in contact with them, temperatures are obtained

that represent the retrograde stage. This finding corroborates the concept that, rather than showing the culmination of metamorphism, the results given by the geothermometers and geobarometers indicate the moment at which the diffusion of Fe and Mg between a mineral pair comes to an end because of the drop in temperature, provided that the temperature was above the blocking temperature of diffusion (Thompson and England 1984, Freer 1981). The blocking temperature recorded by the mineral is affected by grain size and diffusibility in such a way that the blocking temperature is higher for the large grains (Thompson and England *op. cit.*). The lowest temperatures are obtained using the composition of the edge of the garnet and that of the green biotite in contact with it. The temperatures calculated with various methods differ considerably from each other (Table 11). Nevertheless, the highest values correspond to the conditions in the other areas of granulite facies in southern Finland (Korsman 1977, Korsman *et al.* 1984, Schreurs 1985a).

The pressures established are also close to those calculated from the garnet-cordierite barometer



for the crystallization pressures of the areas of granulite facies in southern Finland. The cordierite in contact with the garnet is richer in Mg than in the Sulkava granulite area (Fig. 5), indicating a slightly higher crystallization pressure. The garnet has altered along the edges into cordierite, which may mean that the pressure dropped close to the culmination of metamorphism.

The pressures given by the garnet-plagioclase pair are higher than those given by the garnet-cordierite pair by about one kilobar. This may be due either to the earlier blocking of the barometer or to the fact that the temperature (800°C) used in the calculation was too high, because the slope of the reaction is rather steep. A small garnet grain, 1 mm in diameter, which on the basis of composition represents the retrograde stage, and the plagioclase in contact with it give a clearly lower crystallization pressure than do the cores of the large garnets representing the culmination of metamorphism.

Figure 7 depicts the advance of metamorphism as a function of time based on the reactions between minerals, PT determinations and published datings. Since no relict inclusions that could indicate the evolution of the early prograde

stage have been observed in the minerals of high-grade metamorphism, it is difficult to delineate the advance of the PT path before the culmination of metamorphism. However, nowhere in the migmatite areas of southern Finland nor in their environments has metamorphism of the kyanite type been observed, which means that the rocks probably did not reach the kyanite field during their PT evolution. The cooling path in fig. 7 is supposed to be convex towards the temperature axis. The real situation may be more complex, because the assumption is based only on the rather limited data presented in this study.

The maximum crystallization temperatures and pressures of the granite and garnet-cordierite gneiss are close to each other, indicating that the granite crystallized close to the culmination of metamorphism. The U-Pb ages of titanite and monazite from the trondhjemites in the adjacent Kalanti area are 1810–1845 Ma, which, according to Patchett and Kouvo (1986), are associated with a marked thermal event and reflect the age of metamorphism. The high PT values obtained probably refer to this. The K-Ar age of the biotite from the Heinänen trondhjemite in the Kalanti area is 1718 Ma (sample A493, Lepäinen,

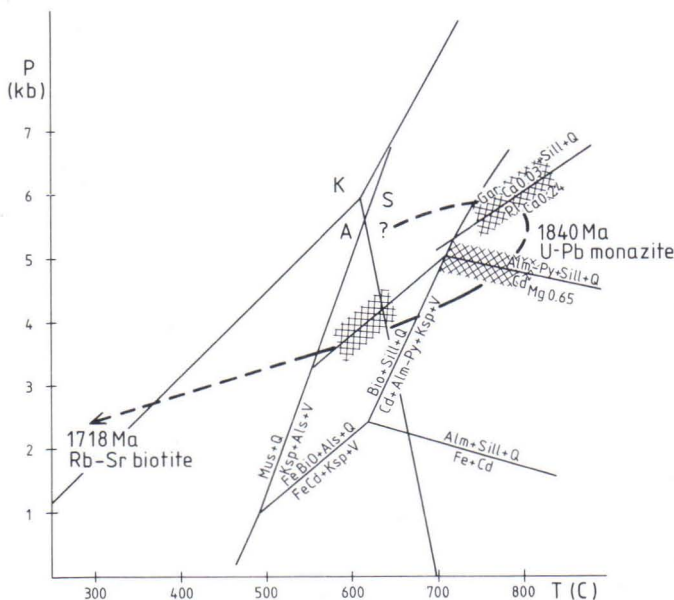


Fig. 7. PT diagram delineating the progress of metamorphism as indicated by the reactions between minerals, the thermobarometers and age determinations. The  $Al_2SiO_5$  triple point after Winkler (1979). The decomposition reactions of muscovite, biotite and cordierite according to Holdaway and Lee (1977), when the partial water pressure was 0.4 of the total pressure.

Patchett and Kouvo 1986). If the age of the biotite represents not a new thermal pulse but cooling, as shown by Fig. 7, this means that uplift has been very slow in the Turku area, provided that cooling was due primarily to erosion and uplift. The far advanced retrograde reactions corroborate the concept of slow cooling.

The metamorphic pressures determined from

the granulite areas of southern Finland are fairly low compared with those from areas of granulite facies on a global scale. All the granulites in the migmatite belt of southern Finland, however, have similar features, i.e. high T, low P and the culmination of metamorphism at a relatively late stage.

### ACKNOWLEDGEMENTS

The present study was undertaken in association with the preparations for the hardrock geological excursion to be arranged in conjunction with the 17th conference of Nordic geologists. The topic was given by Professor Atso Vormaa. The comments by Dr Kalevi Korsman were a

great help in the final stage of the work. The whole-rock analyses were done by Väinö Hoffren and Paula Sarha and the figures were drawn by Ritva Forsman. The manuscript was translated into English by Mrs. Gillian Häkli. To all these persons I express my cordial thanks.

### REFERENCES

- Alapieti, T. & Sivonen, S. J., 1983.** Use of the electron microprobe in the investigation of the early proterozoic Koillismaa layered igneous complex, NE Finland. *Geol. Surv. Finland, Report of Investigation* 61. 22 p.
- Brown, M. & Phadke, A. V., 1983.** High-temperature retrograde reactions in pelitic gneiss from the Precambrian Sausar metasediments of the Ramakona area, Chindwara District, Madhya Pradesh (India): definition of the exhumation P-T-path and the tectonic implications. *J. Geol. Soc India, prof. Kelkar memorial vol.*, 61—96.
- Ferry, J. M. & Spear, F. S., 1978.** Experimental calibration of the partitioning of Fe and Mg between biotite and garnet. *Contr. Mineral. Petrol.* 66, 113—117.
- Freer, R., 1981.** Diffusion in silicate minerals and glasses: a data digest and guide to literature. *Contr. Mineral. Petrol.* 76, 440—454.
- Ganguly, J. and Saxena, S. K., 1984.** Mixing properties of aluminosilicate garnets: constraints from natural and experimental data, and applications to geothermo-barometry. *Am. Min.* 69, 88—97.
- Gorbatshev, R., 1972.** Coexisting varicolored biotites in migmatitic rocks and some aspects of element distribution. *N. Jb. Miner. Abh.* 118 H 1, 1—22.
- Härme, M., 1959.** General geological map of Finland. Pre-Quaternary rocks. Sheet B1, Turku.
- , **1965.** On potassium migmatites of southern Finland. *Bull. Comm. Geol. Finlande* 219. 43 p.
- Hietanen, A., 1943.** Über das Grundgebirge des Kalantigebietes im Südwestlichen Finnland. *Bull. Comm. Geol. Finlande* 130, 106 p.
- , **1947.** Archaean geology of the Turku district in southwestern Finland. *Bull. Geol. Soc. Am.* 58, 1019—1084.
- Hodges, K. V. & Spear, F. S., 1982.** Geothermometry, geobarometry and the  $Al_2SiO_5$  triple point at Mt. Moosilauke, New Hampshire. *Am. Min.* 67, 1118—1134.
- Indares, A. & Martignole, J., 1985a.** Biotite-garnet geothermometry in the granulite facies: the influence of Ti and Al in biotite. *Am. Min.* 70, 272—278.
- Indares, A. & Martignole, J., 1985b.** Biotite-garnet geothermometry in granulite facies rocks: evaluation of equilibrium criteria. *Can. Min.* 23, 187—193.
- Kays, M. A., 1976.** Comparative geochemistry of migmatized, interlayered quartzofeldspathic and pelitic gneisses: a contribution from rocks of southern Finland and north-eastern Saskatchewan. *Precambrian Res.* 3, 433—462.
- Korsman, K., 1977.** Progressive metamorphism of the metapelites in the Rantasalmi—Sulkava area, southeastern Finland. *Geol. Surv. Finland, Bull.* 290. 82 p.

- Korsman, K., Hölttä, P., Hautala, T. & Wasenius, P., 1984.** Metamorphism as an indicator of evolution and structure of the crust in eastern Finland. *Geol. Surv. Finland, Bull.* 328. 40 p.
- Newton, R. C. & Haselton, H. T. I., 1981.** Thermodynamics of the garnet-plagioclase- $\text{Al}_2\text{SiO}_5$ -quartz geobarometer. In Newton et al. (eds), *Thermodynamics of minerals and melts*, New York, Springer-Verlag 131—147.
- Parras, K., 1958.** On the charnockites in the light of a highly metamorphic rock complex in southwestern Finland. *Bull. Comm. Geol. Finlande* 181. 137 p.
- Patchett, J. & Kouvo, O., 1986.** Origin of continental crust of 1.9—1.7 Ga age: Nd isotopes and U-Pb zircon ages in the Svecokarelian terrain of South Finland. *Contr. Min. Petrol.* 92, 1—12.
- Perchuk, L. L. & Lavrentéva I. V., 1983.** Experimental investigation on exchange equilibria in the system cordierite-garnet-biotite. In Saxena S. K. (ed.), *Kinetics and equilibrium in mineral reactions*, New York, Springer-Verlag, 199—239.
- Schreurs, J., 1985a.** The West Uusimaa low pressure thermal dome, SW Finland. PhD Thesis, Free University Amsterdam.
- Schreurs, J., 1985b.** Prograde metamorphism of metapelites, garnet-biotite thermometry and prograde changes of biotite chemistry in high-grade rocks of West Uusimaa, southwest Finland. *Lithos* 18, 69—80.
- Schreurs, J. & Westra, L., 1986.** The thermotectonic evolution of a Proterozoic low pressure, granulite dome, West Uusimaa, SW Finland. *Contr. Min. Petrol.* 93, 236—250.
- Simonen, A., 1980.** The Precambrian in Finland. *Geol. Surv. Finland, Bull.* 304. 58 p.
- Streckeisen, A. & LeMaitre, R. W., 1979.** A chemical approximation to the model QAPF classification of the igneous rocks. *N. Jb. Miner. Abh.* 136, 169—206.
- Thompson, A. B., 1982.** Dehydration melting of pelitic rocks and the generation of  $\text{H}_2\text{O}$ -undersaturated granitic liquids. *Am. J. Sci.* 282, 1567—1595.
- Thompson, A. B. & England, P. C., 1984.** Pressure-temperature-time path of regional metamorphism II. Their inference and interpretation using mineral assemblages in metamorphic rocks. *J. Petrol.* 25, 929—955.
- Vaasjoki, M., 1977.** Rapakivi granites and other postorogenic rocks in Finland: their age and the lead isotopic composition of certain associated galena mineralizations. *Geol. Surv. Finland, Bull.* 294. 64 p.
- Vorma, A., 1976.** On the petrochemistry of rapakivi granite with special reference to the Laitila massif, southwestern Finland. *Geol. Surv. Finland, Bull.* 285. 98 p.
- Westra, L. & Schreurs, J., 1985.** The West Uusimaa complex, Finland: an early Proterozoic thermal dome. In Tobi, A. C. and Touret, J. L. R. (eds), *The deep Proterozoic crust in the North Atlantic provinces*, D. Reidel Publ. Co., 369—380.
- White, A. J. R. & Chappell, B. W., 1983.** Granitoid types and their distribution in the Lachlan fold belt, Southeastern Australia. *Geol. Soc. Am. Mem.* 159, 21—34.

---

**Tätä julkaisua myy**

**VALTION PAINATUSKESKUS  
MARKKINOINTIOSASTO**

**Postimyynti**

PL 516  
00101 HELSINKI 10  
Puh. 90-539 011

**Kirjakauppa**

Annankatu 44  
00100 HELSINKI 10  
Puh. 90-17341

**Denna publikation säljes av**

**STATENS TRYCKERICENTRAL  
MARKNADSFÖRINGSÄVDELNINGEN**

**Postförsäljning**

PB 516  
00101 HELSINGFORS 10  
Tel. 90-539 011

**Bokhandel**

Annegatan 44  
00100 HELSINGFORS 10  
Tel. 90-17341

**This publication can be obtained from**

**GOVERNMENT PRINTING CENTRE  
MARKETING DEPARTMENT**

**Bookshop**

Annankatu 44  
00100 HELSINKI 10  
Phone 90-17341

**Orders from abroad:**

**AKATEEMINEN KIRJAKAUPPA**  
Keskuskatu 1  
SF-00100 Helsinki 10

---

ISBN 951-690-238-3  
ISSN 0367-522X